Published in final edited form as:
J Comp Neurol. 2010 June 1; 518(11): 2071–2089. doi:10.1002/cne.22322.

Progression of Neuronal and Synaptic Remodeling in the *rd10* Mouse Model of *Retinitis Pigmentosa*

M. Joseph Phillips[1], **Deborah C. Otteson**[1], and **David M. Sherry**[2]

[1] University of Houston, College of Optometry, Houston, TX 77204

[2] University of Oklahoma Health Sciences Center, Department of Cell Biology and Oklahoma Center for Neuroscience, Oklahoma City, OK, 73104

Abstract

The *Pde6b*^{rd10} *(rd10)* mouse has a moderate rate of photoreceptor degeneration and serves as a valuable model for human autosomal recessive *retinitis pigmentosa* (*RP).* We evaluated the progression of neuronal remodeling of second- and third-order retinal cells and their synaptic terminals in retinas from *Pde6b*^{rd10} (*rd10*) mice at varying stages of degeneration ranging from postnatal day 30 (P30) to postnatal month 9.5 (PNM9.5) using immunolabeling for well known cell- and synapse-specific markers. Following photoreceptor loss, changes occurred progressively from outer to inner retina. Horizontal cells and rod and cone bipolar cells underwent morphological remodeling that included loss of dendrites, cell body migration, and the sprouting of ectopic processes. Gliosis, characterized by translocation of Müller cell bodies to the outer retina and thickening of their processes, was evident by P30 and became more pronounced as degeneration progressed. Following rod degeneration, continued expression of VGluT1 in the outer retina was associated with survival and expression of synaptic proteins by nearby second-order neurons. Rod bipolar cell terminals showed a progressive reduction in size and ectopic bipolar cell processes extended into the inner nuclear layer and ganglion cell layer by PNM3.5. Putative ectopic conventional synapses, likely arising from amacrine cells, were present in the inner nuclear layer by PNM9.5. Despite these changes, the laminar organization of bipolar and amacrine cells and the ON-OFF organization in the inner plexiform layer was largely preserved. Surviving cone and bipolar cell terminals continued to express the appropriate cell-specific presynaptic proteins needed for synaptic function up to PNM9.5.

Indexing Terms

Photoreceptor degeneration; ribbon synapse; bipolar cell; amacrine cell; plasticity; circuit

Introduction

Retinitis pigmentosa (*RP*) is a degenerative retinal disease characterized by progressive death of rod photoreceptors and affects one in every 2000 individuals worldwide (Sohocki et al., 2001). A genetically heterogeneous disorder, *RP* can result from defects in as many as 100 different genes and can be inherited as an autosomal dominant, autosomal recessive, or X-linked trait, as well as rare mitochondrial or digenic forms (Daiger et al., 2007). Despite the heterogeneous genetic origins of *RP*, the various forms of the disease all share a common phenotype: loss of night and peripheral vision, followed by a progressive loss of

*Correspondence to: Deborah C. Otteson, University of Houston College of Optometry, 4901 Calhoun Rd, J. Davis Armistead Bldg, Houston, TX 77204, Phone: 713-743-1952, Fax: 713-743-2053, dotteson@optometry.uh.edu.

central vision. Although many of the genes that are mutated in patients with *RP* are expressed exclusively in rod photoreceptors, degeneration of rod photoreceptors is typically followed by secondary degeneration of cone photoreceptors (Hartong et al., 2006).

The *Pde6b*^{rd1} (*rd1*) and *Pde6b*^{rd10} (*rd10*) mouse models of *RP* both result from distinct, recessive mutations in the gene encoding the rod-specific, β-phosphodiesterase (*Pde6b*). Mutations in *Pde6b* have also been identified in human patients with autosomal recessive *RP* or congenital stationary night blindness (Hartong et al., 2006). The *rd1* mouse, originally known as the rodless mouse (Keeler, 1924), carries a null mutation that renders the *Pde6b* protein non-functional and homozygotes have an early onset and rapidly progressing degeneration of rod photoreceptors (Bowes et al., 1990; Pittler et al., 1993). Photoreceptor degeneration begins prior to eye opening at postnatal day 14 (P14), with only 2% of rods remaining in the central retina by P17 (Carter-Dawson et al., 1978). The *rd10* mouse carries a missense mutation in *Pde6b* that leaves the phosphodiesterase protein, and therefore rod photoreceptors, with some function. Rod- and cone-driven electroretinograms (ERGs) are present in *rd10* mice when photoreceptor degeneration begins (P18). The ERGs initially show reduced a- and b-wave amplitudes in both dark- and light-adapted conditions compared to wild-type and decline by 90% at 2 months of age (Chang et al., 2007; Gargini et al., 2007). In the *rd10* retina, photoreceptor death peaks at P25 and the outer nuclear layer (ONL) is reduced to a single layer of photoreceptor cell bodies by P35; a small number of cones persist until at least until 9 months of age (Chang et al., 2007; Gargini et al., 2007).

Currently there are no effective treatments for *RP*. Success in restoring vision will rely on the integrity of second- and third-order retinal neurons and their ability to reliably process and transmit visual signals to the brain. However, there is increasing evidence that the death of photoreceptors leads to secondary remodeling of neurons in the remaining retina. This remodeling encompasses a host of negative plastic changes that include loss or sprouting of neuronal processes, loss of glutamate receptors, formation of ectopic synapses, cellular migration and reactive gliosis (Marc and Jones, 2003; Marc et al., 2007). Retinal remodeling has been reported in many animal models of *RP*, across a range of pathologies and etiologies, including the *rd1* and *rd10* mice (Strettoi and Pignatelli, 2000; Strettoi et al., 2003; Gargini et al., 2007; Barhoum et al., 2008; Chua et al., 2009), the Royal College of Surgeons (RCS) rat (Cuenca et al., 2005), and transgenic swine with a mutation in *Rhodopsin* (Banin et al., 1999). Remodeling has also been documented in human *retinitis pigmentosa* (Marc et al., 2007) and age-related macular degeneration (Johnson et al., 2005), as well as in animal models of light-induced retinal damage (Marc et al., 2008) and retinal detachment (Fisher et al., 2005). However, retinal remodeling is not associated exclusively with photoreceptor disease or injury, but also occurs to some degree in glaucoma (Morgan et al., 2006) and in normal aging (Liets et al., 2006; Eliasieh et al., 2007; Terzibasi et al., 2009).

The origins of retinal remodeling in the *rd1* retina are difficult to identify unequivocally, because the early onset results in a significant temporal overlap between degeneration and normal cellular and synaptic development (Blanks et al., 1974; Carter-Dawson et al., 1978; Fisher, 1979; Young, 1985). In contrast, the delayed onset and slower progression of degeneration in the *rd10* mouse retina allows analysis of degeneration and retinal remodeling in the context of a developed and functional retina (Chang et al., 2007; Gargini et al., 2007). The *rd10* mouse is increasingly being used for research to develop new experimental therapies, including rescue through intraocular injection of hematopoietic stem cells (Otani et al., 2004), neuroprotective agents (Boatright et al., 2006; Corrochano et al., 2008; Phillips et al., 2008), antioxidants (Komeima et al., 2007), and gene replacement (Pang et al., 2008). Therefore, increased understanding of the structural, neurochemical, and

functional consequences of remodeling will be important in developing successful interventions and evaluating their effectiveness.

Previous studies have shown that rod bipolar cells and horizontal cells in the retinas of *rd10* mice lose their dendrites by P40 (Gargini et al., 2007; Barhoum et al., 2008; Puthussery et al., 2009), although current information regarding changes in the morphology, size, or complexity of the rod bipolar cell axonal arbors at early stages of degeneration (P45) is contradictory. Given that the loss of photoreceptors results in a progressive decrease in the number of rod bipolar and horizontal cells in the *rd10* retina (Gargini et al., 2007), it is important to determine if and how remodeling progresses at later stages of degeneration and to identify which specific cell types are affected. Other gaps exist in our current understanding of how synapses and circuits remodel, how remodeling progresses in the inner retina and how long the remaining or remodeled synapses retain function. To begin to understand how the inner retinal circuitry remodels, we have evaluated changes in second- and third-order retinal cells and their synaptic terminals in the retinas of homozygous *rd10* mice (ages 1 to 9.5 months) using immunolabeling for specific classes of retinal neurons and their synapses.

Materials and Methods

Animals and tissue preparation

Studies were performed using retinas from homozygous *rd10* mice on a *C57BL/6J* background and from age-matched wild-type *C57BL/6J* mice as controls (both strains from Jackson Laboratories, Bar Harbor, ME). Mice were kept on a 12-hour light: 12-hour dark cycle, with food and water available *ad libitum*. Animals were euthanized by rapid cervical dislocation at the following time points: postnatal day (P) 30, P50, postnatal month (PNM) 3.5, and PNM9.5 (n=3 at each time point). Additional eyes from animals at PNM7.5 and PNM10.5 also were examined. Following enucleation, the cornea and lenses were removed and the eyes were immersion fixed in 4% paraformaldehyde in 0.1M cacodylate buffer (pH 7.4) for 1 hour at 4°C. Eyecups were rinsed in Hank's Balanced Salt Solution (HBSS, pH 7.4), cryoprotected overnight in 30% sucrose in HBSS, embedded in Optimal Cutting Temperature medium (O.C.T.; Sakura Tissue Tek; VWR, West Chester, PA), and flash frozen in liquid nitrogen. Frozen sections (10–14 μm thickness) were collected on Superfrost Plus slides (Fisher Scientific, Pittsburgh, PA) and stored at −20°C until use. All animal procedures conformed to US Public Health Service and Institute for Laboratory Animal Research guidelines and were approved by the University of Houston Institutional Animal Care and Use Committee.

Antibody Characterization

An extensive panel of well-characterized antibodies against cell- and synapse-specific markers was used for single-, double- and triple-labeling studies. Table 1 contains a complete list of antibodies, immunogens, manufacturers, host species and dilutions used. Immunostaining patterns in the retina have been previously described for all antibodies and, in our hands, all antibodies stained the appropriate cell types and showed the expected distribution in retinas from C57Bl/6 mice.

1. Calbindin mouse monoclonal and rabbit polyclonal antibodies recognize a single band of 28 kDa in Western blots of brain homogenates from wild-type mice, but no bands in blots from calbindin knockout mice (Celio et al., 1990; Airaksinen et al., 1997). The monoclonal and polyclonal antibodies against calbindin used in these studies showed the same pattern of staining in the mouse retina that has previously been shown to be horizontal cells and cholinergic amacrine cells and their processes (Haverkamp and Wässle, 2000).

2. Calretinin rabbit polyclonal antibodies recognize a single, 35 kDa spot on Western blots of 2-dimensional isoelectric focusing gels of guinea pig cerebellum; immunoreactivity to histological sections of guinea pig cerebellum is eliminated by preabsorption of antibodies with 1 μM purified calretinin (Winsky et al., 1989). The anti-calretinin antibodies used in these studies showed the same pattern of staining in the mouse retina that has previously been identified as starburst and TH2 amacrine cells (Haverkamp and Wässle, 2000).

3. Glutamic Acid Decarboxylase (GAD-65) rabbit polyclonal antibodies recognize two bands, 65 and 67 kDa, on Western blots of mouse brain lysates (manufacturer's technical information (Belichenko et al., 2009). The anti-GAD-65 antibodies used in this study showed the same staining pattern in the mouse retina that previous studies have identified as GABAergic amacrine cells (Haverkamp and Wässle, 2000)

4. Gγ13 rabbit polyclonal antibodies recognize a ~8 kDa band in mouse olfactory epithelium (Kerr et al., 2008). Immunoreactivity to murine lingual tissue is blocked by preincubation with 1 μM of the synthetic peptide immunogen (Huang et al., 1999). Gγ13 antibodies used in this study showed the same staining pattern in the mouse retina that previous studies have identified as ON bipolar cells (rod and cone) (Huang et al., 2003).

5. Ionotropic glutamate receptor subunit 4 (GluR4) rabbit polyclonal antibodies recognize a single band of 100 kDa on Western blots of rat brain and in COS-7 cells transfected with a GluR4 cDNA construct, but not in COS-7 cells transfected with GluR1, GluR2 or GluR3 (Wenthold et al., 1992). The anti-GluR4 antibodies used in this study showed the same pattern of staining in the mouse retina that previous studies have identified as horizontal and OFF-cone bipolar cells (Haverkamp and Wässle, 2000).

6. Glutamine synthetase (GS) mouse monoclonal antibody recognizes a single 45 kDa band on Western blots of sheep and rat brain (manufacturer's information). The GS antibody used in this study showed the same staining pattern in the mouse retina that previous studies have identified as Müller glia (Haverkamp and Wässle, 2000).

7. Protein kinase C-α (PKCα) polyclonal and monoclonal antibodies recognize a single 82 kDa band on Western blots of total proteins from rat brain; immunohistochemical staining is abolished with the immunizing peptide (manufacturers' information). The monoclonal and polyclonal antibodies against PKCα used in this study showed the same staining pattern in the mouse retina that previous studies have identified as rod bipolar cells (Haverkamp and Wässle, 2000; Ghosh et al., 2004).

8. SNAP-25 mouse monoclonal antibody recognizes a single band at 25 kDa on Western blots of rat cerebral cortices (Garbelli et al., 2008). The SNAP-25 antibody used in this study showed the same staining pattern in the mouse retina that previous studies have identified as all synapses (Greenlee et al., 2001).

9. Synaptic vesicle protein 2 (SV2) mouse monoclonal antibody cross reacts with all three SV2 isoforms and recognizes a large, diffuse band at ~90 kDa on Western blots of mouse brain membranes (Buckley and Kelly, 1985); in SV2A and SV2B double knockout mice, immunoreactivity is reduced to a very faint band, reflecting remaining SV2C (Lynch et al., 2004). The pan SV2 monoclonal antibody used in this study showed the same staining pattern in the mouse retina that previous studies have identified as all synapses (Wang et al., 2003).

10. Synapsin 1 mouse monoclonal antibody recognizes a doublet consisting of synapsin 1a and 1b at ~80 kDa band in Western blots of total homogenates and membrane fractions of mouse forebrain (Martínez et al., 1998). The synapsin 1 antibody used in this study showed the same staining pattern in the mouse retina that previous studies have identified as conventional synapses (Sherry et al., 2006).

11. Syntaxin 3 rabbit polyclonal antibodies recognize a single 35–36 kDa band in Western blots of mouse retina and brain. The anti-syntaxin 3 polyclonal antibodies used in this study showed the same staining pattern in the mouse retina that previous studies have identified as ribbon synapses (Sherry et al., 2006).

12. Syntaxin 4 rabbit polyclonal antibodies recognize a single band of 36 kDa on a Western blot of retina and brain homogenates; preabsorption with the peptide immunogen eliminates labeling. The syntaxin 4 polyclonal antibodies used in this study showed the same staining pattern in the mouse retina that previous studies have identified as horizontal and amacrine cells (Sherry et al., 2006).

13. Tyrosine Hydroxylase (TH) mouse monoclonal antibody recognizes a 59–61 kDa band in Western blots of mouse brain lysates and does not react with dopamine-beta-hydroxylase, phenylalanine hydroxylase, tryptophan hydroxylase, dehydropteridine reductase, sepiapterin reductase or phenethanolamine-N-methyl transferase (manufacturer's information). The monoclonal antibody against TH used in this study showed the same staining pattern in the mouse retina that previous studies have identified as dopaminergic amacrine cells (Haverkamp and Wässle, 2000; Zhang et al., 2005).

14. Vesicle associated membrane protein-2 (VAMP-2) rabbit polyclonal antibodies recognize a 19 kDa band on Western blots of total proteins from mouse brain and retina (Sherry et al., 2003b). The 19 kDa band labeled by VAMP-2 antibodies in Western blots of total protein lysates of cultured neurons from embryonic day 18 (E18) wild-type mice was absent in lysates of neurons cultured from E18 VAMP-2 knockout mice (Schoch et al., 2001). Polyclonal anti-VAMP-2 antibodies used in this study showed the same staining pattern in the mouse retina that previous studies have identified as all synapses (Sherry et al., 2003b).

15. Vesicular glutamate transporter 1 (VGluT1) guinea pig polyclonal antibodies recognize a 60 kDa band on Western blots of synaptic membrane fractions from rat cerebral cortex (Melone et al., 2005); preabsorption with the immunogen peptide abolishes immunostaining (manufacturer's information). Polyclonal anti-VGluT1 antibodies used in this study showed the same staining pattern in the mouse retina that previous studies have identified as ribbon synapses (Bellocchio et al., 1998; Sherry et al., 2003a).

16. Vesicular glutamate transporter 3 (VGluT3) guinea pig polyclonal antibodies recognize a doublet migrating at ~60–62 kDa in Western blots of rat astrocytes and preabsorption with the immunizing peptide abolishes staining in Western blots (Montana et al., 2004) and immunohistochemistry (manufacturer's information). The polyclonal anti-VGluT3 antibodies used in this study showed the same staining pattern in the mouse retina that previous studies have identified as glutamatergic amacrine cells (Haverkamp and Wässle, 2004; Johnson et al., 2004).

Secondary antibodies were raised in goat against IgGs from rabbit, mouse, guinea pig, or mouse IgM. Secondary antibodies were conjugated to Cy3 or Cy5 (Jackson Immunoresearch Laboratories, West Grove, PA), or to AlexaFluor488, AlexaFlour543, or AlexaFluor633 (Molecular Probes, Eugene, OR) and were used at a dilution of 1:200.

Immunolabeling and Imaging

Immunolabeling and imaging of cryosections were performed according to previously published protocols (Sherry et al., 2006). Briefly, cryosections were thawed, incubated in 1% $NaBH_4$ for 2 minutes to reduce autofluorescence prior to incubation in blocker (10% normal goat serum or 2% donkey serum, 5% bovine serum albumin, 1% fish gelatin, 0.5% Triton X-100 in HBSS, pH 7.4) for 2 hours at room temperature to reduce non-specific labeling. After removing the blocker, the primary antibody or a combination of primary antibodies from different hosts diluted in blocker was applied for 2 days at 4°C. Sections were rinsed, incubated in secondary antibodies for 1 hour at room temperature, rinsed extensively and then coverslipped using Prolong Gold (Molecular Probes, Eugene, OR) to retard bleaching of the fluorescent labels. Specificity of labeling methods was confirmed by omitting primary antibody or by substituting normal serum from the species used to generate the specific primary antiserum. Labeling of additional specimens using only one primary antibody in combination with multiple secondary antibodies confirmed the absence of secondary antibody cross-reactivity and bleed-through of signals between fluorescence channels.

Confocal microscopy was performed using a Leica TCS-SP2 confocal microscope (Leica Microsystems, Exton, PA). Images were captured using a 63X oil immersion objective (N.A. 1.32) and frame-averaged to reduce noise. Bleed-through between fluorescence channels was eliminated by scanning channels sequentially and adjusting laser power and detector sensitivity. In all cases, image scale was calibrated, and brightness and contrast were adjusted if necessary to highlight specific labeling. To assess double- and triple-labeling, matching images in the AlexaFluor488, Cy3/AlexaFlour543, or Cy5/AlexaFluor633 channels were captured independently, pseudo-colored green and magenta for double-labeled specimens, or green, red, and blue for triple labeled specimens and superimposed using Photoshop software (Adobe Systems, San Jose, CA).

Results

VGluT1 in photoreceptor and bipolar cell terminals

VGluT1 is responsible for loading glutamate in synaptic vesicles and is a marker for rod and cone photoreceptor terminals in the outer plexiform layer (OPL) and bipolar cell terminals in the inner plexiform layer (IPL) (Sherry et al., 2003a). In the wild-type retina, the VGluT1-positive synaptic terminals of photoreceptors form a continuous band in the OPL at all ages (Fig. 1A, D). As photoreceptor cells degenerated in the *rd10* retina, the number of VGluT1-immunoreactive puncta in the OPL decreased, reflecting the loss of photoreceptor terminals (Fig. 1B, C, E, F). At P30 and P50, the plexus of VGluT1-positive terminals in the OPL was reduced and discontinuities became evident (Fig. 1B, C). With time, the remaining sites of VGluT1 staining in the OPL became more widely spaced (Fig. 1E) and by PNM9.5, VGluT1 immunoreactivity in the OPL was largely absent (Fig. 1F). However, even at this advanced stage of degeneration, a few sites of VGluT1 staining persisted in the OPL.

In contrast to the rapid loss of VGluT1 labeling in the OPL, changes in VGluT1 labeling of bipolar cell terminals in the IPL were more subtle, particularly at early timepoints. VGluT1-positive, rod bipolar terminals are much larger than cone bipolar terminals and stratify in the innermost portion of the IPL, making them easily identifiable in both wild-type (Fig. 1A, D) and *rd10* retinas at P30 (Fig. 1B). However, even at this early stage of degeneration, the pattern of VGluT1 immunoreactivity associated with rod bipolar terminals appeared disorganized in the *rd10* retinas. The plexus of large VGluT1-positive rod bipolar terminals in the innermost IPL was substantially reduced by P50 (Fig. 1C) and could not be distinguished morphologically from VGluT1-positive cone-bipolar terminals at advanced

stages of degeneration [PNM3.5 (Fig. 1E) and PNM9.5 (Fig. 1F)]. It is important to note, however, that VGluT1-positive bipolar cell terminals were present throughout the IPL even at advanced stages of degeneration.

Rod Bipolar Cells

Protein kinase C-α (PKCα) is a marker for mouse rod bipolar cells (Haverkamp and Wässle, 2000) and antibodies against PKCα revealed the expected morphology of wild-type rod bipolar cells: fine dendrites that project distally to rod terminals, a row of cell bodies in the distal inner nuclear layer (INL), and large, lobular axon terminals that stratify in the innermost portion of the IPL (Fig. 2A, PNM3.5 shown). In wild-type retinas, this pattern of immunostaining remained unchanged from P30 to PNM9.5. In the *rd10* retina, in addition to the loss of fine dendritic processes that has been previously reported at early timepoints (Gargini et al., 2007; Barhoum et al., 2008; Puthussery et al., 2009), we also found that by PNM3.5, surviving PKCα-positive, rod bipolar cells were often found in clusters. Rod bipolar cell clusters were specifically associated with the few remaining sites of VGluT1 immunoreactivity (Fig. 2B, F) and bipolar cells occasionally extended short, thickened processes towards these VGluT1-positive sites (Fig. 2B, F).

Previous reports are contradictory as to whether rod bipolar cell axon terminals also remodel (Gargini et al., 2007; Barhoum et al., 2008). We observed a progressive reduction in the size of the VGluT1-positive puncta in the innermost IPL that suggested that rod bipolar cell terminals remodeled or were lost as degeneration progressed (Fig. 1B, C, E, F). In sections of *rd10* retinas double-stained for PKCα and VGluT1 at PNM3.5, rod bipolar axon terminals in the IPL were clearly present and retained expression of VGluT1, albeit at a reduced level (Fig. 2F). Ectopic, PKCα-positive processes also were present in the inner nuclear layer (INL) and ganglion cell layer (GCL) in the *rd10* retina (Fig. 2B), although most of these ectopic processes showed little VGluT1 immunoreactivity (Fig. 2F).

ON-bipolar cells

Gγ13 is a guanine nucleotide-binding protein and is part of the heterotrimeric G-protein complex coupled to mGluR6 (Huang et al., 2003). Antibodies against Gγ13 label both rod and ON-cone bipolar cells from their dendrites to their axon terminals (Fig. 3A). In the *rd10* retina, consistent with the known remodeling of PKCα-positive, rod bipolar cell dendrites (Gargini et al., 2007; Puthussery et al., 2009), the plexus of Gγ13-positive rod and ON-cone bipolar dendrites in the OPL became disorganized by P30 (Fig. 3G). The thin ascending dendrites that normally contact photoreceptor terminals were notably reduced and remaining dendrites appeared abnormally thickened (Fig. 3G). Despite the loss of fine dendritic processes, the Gγ13-positive plexus of ON bipolar dendrites extended throughout the OPL with few discontinuities at P30 and remained closely associated with VGluT1 immunoreactivity (Fig. 1G–I). This staining pattern was consistent with the continued presence of ON-cone bipolar cell dendrites. By PNM3.5 the dendrites of both rod and ON-cone bipolar cells were largely absent from the OPL (data not shown). By PNM9.5, the Gγ13-positive dendritic plexus in the OPL had disappeared, except for large dense patches that were associated with the remaining sites of VGluT1 immunoreactivity (Fig. 3J-L). Double staining with Gγ13 and PKCα showed that the clusters of Gγ13-positive cells consisted of both rod bipolar cells (PKCα-positive/Gγ13-positive) and ON-cone bipolar cells (PKCα-negative/Gγ13-positive) (Fig. 3P–R). Thus, degeneration of photoreceptors in the *rd10* retina affected the dendritic organization of both rod bipolar and ON cone bipolar cells.

Stratification of ON and OFF bipolar cell terminals

Double labeling for Gγ13 and VGluT1, combined with morphological features, allows identification of OFF-cone, ON-cone, and rod bipolar cell terminals and reveals their

stratified organization within the IPL (Fig. 3A–F). In the wild-type retina, OFF-cone bipolar cell terminals are labeled by antibodies against VGluT1, but not Gγ13, and normally terminate in the distal 40% of the IPL (Fig. 3C, F). ON-cone bipolar and rod bipolar cell terminals are immunopositive for both VGluT1 and Gγ13, but can be distinguished by position and size. The small terminals of ON-cone bipolar cells normally terminate in the inner 60% of the IPL, just distal to the large rod bipolar terminals that occupy the innermost region of the IPL (Fig. 3A, D). In *rd10* retinas at P30, the stratified ON-OFF organization of bipolar cell terminals in the IPL was still intact (Fig. 3G–I) and remained largely undisturbed until at least PNM9.5 (Fig. 3J–L). At PNM3.5 and later, Gγ13-positive terminals remaining in the IPL were still largely confined to the ON sublamina, as appropriate (Fig. 3J–L). Importantly, the terminals of both ON- and OFF-cone bipolar cells continued to express VGluT1, even at advanced stages of degeneration, suggesting that they may retain the ability to release glutamate. However, some remodeling of ON bipolar cells did occur, as small, spray-like processes showing labeling for Gγ13 were observed in the OFF sublamina at advanced stages of degeneration (arrowheads, Fig. 3J–L). Occasional ectopic Gγ13-positive processes also projected into the GCL at PNM9.5 and showed distinct co-localization with VGluT1 (Fig. 3L). In contrast, ectopic Gγ13-positive processes in the outermost IPL showed no co-localization with VGluT1.

Although double-labeling for VGluT1 and PKCα revealed that rod bipolar cell terminals persisted at late stages of degeneration, few of the Gγ13-positive/VGluT1-positive puncta in the IPL could be identified as rod bipolar cell terminals on the basis of morphology alone by PNM9.5 (Fig. 3L). However, double-staining for Gγ13 and PKCα confirmed the presence of a reduced, but distinct sublamina of rod bipolar cell terminals in the innermost IPL that was appropriately located proximal to the Gγ13-positive/PKCα-negative terminals of the ON-cone bipolar cells (Fig. 3R).

Horizontal cells

There is a single horizontal cell type in the mouse retina that can be labeled using antibodies against calbindin (Haverkamp and Wässle, 2000). Mouse horizontal cells synapse with cone terminals via the dendrites and with rod terminals via the axon (Peichl and González-Soriano, 1994). In the retinas of wild-type mice, the fine processes of the horizontal cells invaginate into the terminals of rods and cones and, when stained with antibodies against calbindin, appear as small distinct puncta in the OPL at all ages (Fig. 4A, D). In addition to the previously described loss of dendritic complexity at early stages of degeneration (Gargini et al., 2007; Barhoum et al., 2008; Puthussery et al., 2009), some horizontal cell bodies migrated into the ONL and ectopic calbindin-positive processes extended into both the INL and ONL at P30 (Fig. 4). By P50, the fine processes of horizontal cells in the OPL had largely disappeared and progressively fewer ectopic calbindin-positive cell bodies and processes were detected as degeneration progressed (Fig. 4C, E, F). As photoreceptor degeneration progressed, horizontal cells located near sites of VGluT1 immunoreactivity in the OPL selectively maintained their processes and expression of the SNARE protein, syntaxin 4 (Fig. 5K, L, N, O). Some horizontal cells that maintained dendritic processes also continued to express the AMPA glutamate receptor subunit, GluR4 (Supplemental Fig. 1).

Stratification of third-order amacrine cells

The processes of many subtypes of amacrine cells form precise strata in the IPL that can be identified using specific antibodies. In addition to horizontal cells, antibodies against calbindin stain cholinergic amacrine cells and three distinct strata in the IPL that contain their dendrites (Haverkamp and Wässle, 2000) (Fig. 4A, D). Stratification of calbindin-positive amacrine cell processes was preserved in the *rd10* retina at PNM9.5 (Fig. 4F). To further examine the distribution of the processes of several highly stratified amacrine cell

types, we used immunolabeling for VGluT3, GAD-65, TH, and calretinin. Antibodies against VGluT3 label the processes of a putative glutamatergic amacrine cell type that stratifies in the middle of the IPL (Fig. 6A). The normal pattern of stratification was maintained in the *rd10* retina at all ages examined, including PNM9.5 (Fig. 6B). Although VGluT3 immunoreactivity appeared slightly reduced at PNM9.5, this was not consistent across specimens. GAD-65 catalyzes formation of gamma-aminobutyric acid (GABA) from L-glutamic acid and is a marker for GABAergic amacrine cells. In the wild-type retina, antibodies against GAD-65 labeled three prominent strata in the IPL that are separated by unstained strata containing the terminals of the cholinergic starburst amacrine cells (Fig. 6C). Again, no consistent changes in the distribution of GAD-65 were observed in the retinas of *rd10* mice at PNM9.5, suggesting that GABAergic amacrine cell organization was largely preserved (Fig. 6D). In both wild-type and *rd10* retinas, VGluT3 immunoreactivity co-stratified with the middle, GAD-65 plexus, as appropriate (Fig. 6E, F).

Double labeling for TH and calretinin was used to assess the organization of additional amacrine cell types. Antibodies against TH label type-1 dopaminergic amacrine cells that stratify at the INL/IPL border. In both wild-type and *rd10* retinas, TH-positive processes stratified appropriately, distal to the calretinin-positive strata of the cholinergic starburst amacrine cells (Fig. 6G, H). However, the TH stratum was more diffuse in the *rd10* retinas than the wild-type retina. Antibodies against calretinin label the ON and OFF starburst amacrine cell plexes in the IPL, plus a third amacrine cell type that stratifies at the border of the ON and OFF sublaminae. The normal pattern of calretinin-positive amacrine cell stratification was observed in the retinas of both wild-type and *rd10* mice. Although three calretinin-positive strata persisted in the *rd10* retina, they were appreciably more diffuse at PNM9.5, particularly the outermost, OFF-starburst amacrine cell plexus. These results suggest that the ON/OFF stratification of third-order amacrine cells remains largely intact even at stages of advanced photoreceptor loss.

Expression of presynaptic proteins

In advanced *RP*, assessment of synaptic integrity and function in the inner retina of retinas is difficult because of the loss of light-evoked activity that occurs with severe photoreceptor degeneration. Previous studies showed that in *rd10* retinas, ribbon synapses in cone pedicles are still present in the OPL until at least P20 (Puthussery et al., 2009). If the continued expression of VGluT1 that we observed in the OPL is indicative of functional synaptic terminals, other presynaptic proteins associated with neurotransmitter release also should be present in surviving photoreceptor terminals. To examine expression of presynaptic proteins associated with neurotransmitter release by photoreceptors and bipolar cells, we used antibodies against presynaptic proteins that are expressed in ribbon synapses.

Sections were immunostained with antibodies against the SNARE proteins, SNAP-25 or VAMP-2, in conjunction with markers for bipolar cells and ribbon synapses (i.e., PKCα and VGluT1 in Fig. 7). Staining for SNAP-25 in the OPL was prominent in *rd10* retinas at PNM9.5 and the remaining sites of VGluT1 staining in the OPL were localized within the SNAP-25-positive plexus (Fig. 7D). In both *C57BL/6* and *rd10* retinas at PNM9.5, there was also strong staining for SNAP-25 in the IPL that co-localized with VGluT1 (Fig. 7C–H). PKCα-positive terminals of rod bipolar cells were also positive for both VGluT1 and SNAP-25 (Fig. 8G, H).

In the wild-type retina, antibodies against syntaxin 3 stained the plasma membranes and terminals of photoreceptors in the outer retina and bipolar cells in the inner retina. In addition, syntaxin 3 labeling specifically co-localized with VGluT1 immunoreactivity in the synaptic terminals of photoreceptor and bipolar cells (Fig. 8A–C). In the *rd10* retina at P30, the loss of photoreceptors is evident by reduced syntaxin 3 labeling in the ONL and the

thinning of the plexus of photoreceptor terminals in the OPL (Fig. 9D). However, it appeared that all surviving photoreceptor terminals in the OPL continue to co-express syntaxin 3 and VGluT1 at P30 (Fig. 8F). By PNM9.5, there were obvious discontinuities in the syntaxin 3-positive plexus in the OPL. Although VGluT1 staining in the outer retina of the rd10 retina was more restricted at PNM9.5, VGluT1-positive puncta in the OPL were located within the syntaxin 3-positive plexus (Fig. 8G–I). VGluT1 staining in the IPL became more diffuse in the *rd10* retina at PNM9.5, although VGluT1 immunoreactivity in the IPL continued to show extensive co-localization with syntaxin 3.

The conventional synapses of amacrine cells also maintained appropriate expression of presynaptic proteins associated with neurotransmitter release. In wild-type retina, syntaxin 4 is expressed in some amacrine cell boutons in the IPL (Fig. 5D). Syntaxin 4 expression in the IPL was largely unaffected by the advanced photoreceptor degeneration in *rd10* retinas at PNM9.5. Double labeling for VAMP-2, the principle synaptic vesicle SNARE in retinal synapses, and SV2, using a pan-specific antibody that recognizes all SV2 isoforms, showed a relatively normal pattern of VAMP-2 and SV2 co-localization throughout the IPL of the *rd10* retina at PNM9.5 (Fig. 9D–F). In the INL, there was increased ectopic expression of VAMP-2 and SV2 that showed extensive co-localization in the *rd10* retina at PNM9.5 (Fig. 9D–F).

Synapsin 1 is a synaptic vesicle protein present only in conventional amacrine cell synapses. In the IPL, synapsin 1 immunoreactivity co-localized with only a subset of VAMP-2-positive terminals, consistent with VAMP-2 labeling of conventional synapses as well as bipolar cell terminals in both wild-type and *rd10* retinas (Fig. 9G–L). In the PNM9.5 *rd10* retina, immunoreactivity for synapsin 1 was also present in discrete puncta in the INL and GCL and co-localized with many sites of VAMP-2 expression.

Müller glia

Apart from upregulation of glial fibrillary acidic protein (GFAP) in Müller glia in the *rd10* retinas at P20 and P60, the only reported change in Müller glial morphology is a reduction in the length of distal processes associated with the loss of photoreceptors in the ONL (Gargini et al., 2007). Because most photoreceptor degenerations trigger the formation of glial scars, we looked for evidence of gliosis in the *rd10* retina at later stages of degeneration. Antibodies against GS label the entirety of the Müller cell including the soma, processes and endfeet at the inner and outer limiting membranes. In the retinas of wild-type mice, staining for GS revealed a row of irregularly shaped Müller cell bodies in the middle of the INL from P30 to PNM9.5 (Fig. 10A-C). In the retinas of *rd10* mice, beginning as early as P30 and continuing until PNM9.5, a discrete row of Müller cell bodies was no longer detectable in the INL (Fig. 10D–F). Instead, Müller cell bodies translocated to the outermost region of the INL and were occasionally observed in the outer retina. In *rd10* mice, the Müller cell processes around the remaining photoreceptor cell bodies in the ONL became thicker. Strong GS immunoreactivity and thickened Müller cell processes were apparent around remaining cells in the outermost retina until at least 9.5 months (arrowheads, Fig. 10F).

Discussion

Following photoreceptor degeneration in the *rd10* mouse, many of the remaining retinal neurons undergo progressive remodeling. Our results extend previous studies of retinal degeneration and remodeling in the *rd10* mouse (Chang et al., 2007; Gargini et al., 2007; Barhoum et al., 2008; Mazzoni et al., 2008) by documenting the sequence of changes to an advanced stage of degeneration (PNM9.5), roughly 8 months after the complete loss of rod photoreceptors. In contrast to previous results (Gargini et al., 2007), we find gliotic changes in Müller glia as early as P30. Our results address conflicting reports regarding remodeling

of rod bipolar terminals (Gargini et al., 2007; Barhoum et al., 2008) by showing the progressive changes in the morphology, but not the stratification, of VGluT1 expressing rod bipolar cell terminals. Our analysis also extends previous studies by documenting expression patterns of additional proteins necessary for synaptic function. Importantly, despite the significant remodeling that occurs in the outer retina, our results show that the ON/OFF stratification and the expression of synaptic proteins necessary for presynaptic function of second and third-order neurons in the IPL are largely preserved. Thus, if lost photoreceptors can be replaced and successfully reconstitute functional synapses with the second-order neurons in the OPL, the inner retina is likely to retain the potential for functionally appropriate visual processing. Continued expression of the postsynaptic machinery also would be needed to maintain visual processing in the inner retina. Although further analyses are needed, recent studies in the degenerating retina using 1-amino-4-guanidobutane (AGB, agmatine), a guanidinium analog that selectively passes through activated glutamate-gated channels, suggest that expression of key post-synaptic proteins in the IPL is maintained (Marc et al., 2007).

Second-order neurons (bipolar and horizontal cells) showed the most dramatic changes following photoreceptor degeneration. Previous studies have shown that as photoreceptors die in the *rd10* mouse retina, nearly a quarter of rod bipolar cells are also lost (Gargini et al., 2007). We find that at PNM3.5 and PNM9.5, surviving rod and ON-cone bipolar cells in the *rd10* retinas are located in clusters that likely correspond to the rosette-like, circular domains of PKCα-positive rod-bipolar cells observed by Gargini *et al.* (2007). Rod bipolar cells that survived until PNM9.5 typically extended processes towards the few remaining sites of VGluT1 immunoreactivity in the OPL. Cone degeneration in the *rd10* retina is slower than rod degeneration, with some cones persisting to at least 9 months (Gargini et al., 2007). Therefore, the remaining VGluT1 immunoreactivity in the OPL most likely represents the terminals of surviving cone photoreceptors. Abnormal association of rod bipolar cell dendrites with ribbon synapses of cone pedicles has been shown using immuno-electron microscopy at P20 (Puthussery et al., 2009) and our results suggest that the association between rod bipolar cells dendrites and surviving cone photoreceptor terminals is likely to persist, even at late stages of degeneration.

Horizontal cells also remodeled extensively following photoreceptor cell death, consistent with previous reports (Gargini et al., 2007; Barhoum et al., 2008). In addition to the loss of dendritic processes and extension of ectopic projections into the INL, we found that horizontal cells adjacent to remaining sites of VGluT1 and syntaxin 4 immunoreactivity in the OPL consistently retained some dendritic processes. Expression of the SNARE protein SNAP-25 in the outer retina was higher than expected, given the sparse distribution of surviving cones at late stages of degeneration. The localization of SNAP-25 could reflect errors in protein trafficking or aberrant attempts by second-order neurons to generate new synapses in the absence of presynaptic input. Alternatively, SNARE proteins can serve other membrane trafficking functions (Zhou et al., 2000; Hepp and Langley, 2001) and the high expression levels in the outer retina could point to a role for these proteins in glial scar formation. However, syntaxin 3 and SNAP-25 showed little co-localization with the Müller cell marker GS (data not shown), suggesting that expression of syntaxin 3 and SNAP-25 was neuronal rather than glial.

The association of the rod bipolar and horizontal cell processes with the remaining sites of VGluT1 in the OPL suggests that surviving cones may provide trophic support that locally enhances survival of post-synaptic cells and their dendritic processes. Glutamate is an excellent candidate, as many of the synaptic proteins necessary for glutamate release from surviving cone terminals continue to be expressed as degeneration proceeds. Consistent with the survival of some functional cone terminals, double labeling studies have shown

appropriate co-localization of many synaptic proteins including VGluT1, syntaxin 3, VAMP-2, and SV2 (this study) and the synaptic ribbon protein CtBP2 (Puthussery et al., 2009), even at late stages of degeneration.

Although evidence for glutamate release by surviving cones is indirect, there is evidence that bipolar cells in the degenerating retina are capable of responding to glutamate. Expression of mGluR6, the metabotropic glutamate receptor in rod bipolar and ON-type cone bipolar cells persists until P45 in the *rd10* retina (Gargini et al., 2007; Barhoum et al., 2008; Puthussery et al., 2009) and expression of ionotropic glutamate receptors (GluR1, GluR2, and GluR4) persists in the OPL until at least P180 (Puthussery et al., 2009). More importantly, exogenous glutamate can elicit ionic currents in isolated rod and cone bipolar cells and in slices from *rd10* retinas at P60 (Barhoum et al., 2008; Puthussery et al., 2009). We found that GluR4 expression was co-localized with calbindin in some horizontal cells at late as PNM9.5, suggesting that second-order neurons, particularly those located near surviving cone terminals, retain the ability to respond to glutamatergic input even at late stages of degeneration. Interestingly, despite the striking gliotic changes in Müller cells that occured as photoreceptor degeneration progressed, Müller cells continued to express GS, a key enzyme for glutamate metabolism. Taken together, the evidence supports a potential role for photoreceptor input in the maintenance of glutamate receptor expression and survival of post-synaptic cells in the degenerating retina.

The close association of the bipolar cell and horizontal cell dendrites with the putative surviving cone terminals raises the question of whether second- and third-order neurons in the degenerating retina retain the synaptic machinery necessary to transmit a signal. Previous reports are contradictory regarding remodeling of rod bipolar cell terminals in the *rd10* retinas at P40-P45, with one group reporting no changes (Gargini et al., 2007) and the other showing a reduction in size and loss of PKCα immunoreactivity in rod bipolar cell axon terminals at P40 (Barhoum et al., 2008). Our results show a progressive loss in size of rod bipolar cell terminals, with initial disorganization apparent as early as P30. Despite the morphological changes, rod bipolar cells continue to express VGluT1, the critical vesicular transporter needed to load glutamate into synaptic vesicles for release, as late as PNM9.5, albeit at reduced levels. The potential that these cells retain the ability to transmit synaptically is supported by the continued expression and co-localization of other key synaptic proteins normally associated with rod and cone bipolar cell ribbon synapses and conventional amacrine cell synapses in the IPL at PNM9.5. Consistent with this, spontaneous glutamatergic neurotransmission in the IPL, presumably from bipolar cells, persists in late-stage photoreceptor degeneration in the retinas of rodless-coneless *(rdcl)* mice, *hrhoG* transgenic mice, and in human *RP* (Marc et al., 2007). Although transmission by amacrine cells has not been investigated directly in retinas with late stage photoreceptor degeneration, surviving amacrine cells retain their cell-specific amino acid neurotransmitter signatures, even in extremely advanced degeneration (Marc et al., 2003; Jones and Marc, 2005).

The basic ON-OFF stratification of the IPL is retained in the *rd10* retina until at least PNM9.5, as evidenced by the preservation of the appropriate stratification of bipolar cells axon terminals in the ON and OFF sublaminae within the IPL. Even at advanced stages of photoreceptor degeneration, we find that third-order amacrine cells maintain relatively normal, cell-specific dendritic stratification in the IPL. This observation extends to all classes of amacrine cells examined, including five distinct classes of amacrine cells (GABAergic, VGluT3, dopaminergic, ON and OFF starburst, and an additional calretinin-positive type). The continued maintenance of the functional segregation of the ON and OFF pathways and amacrine cell stratification may contribute to the long term survival of retinal

ganglion cells and the high degree of preservation of their dendritic structure and axonal projections observed in *rd10* mice at 9 months of age (Mazzoni et al., 2008).

Although a great deal of inner retinal circuitry appears to be preserved for long periods following photoreceptor degeneration, there is evidence for some remodeling in the inner portion of the *rd10* retina. In particular, amacrine cells stratifying in the OFF sublamina of the IPL appear to be somewhat more sensitive to the loss of light-driven photoreceptor input, as the plexes of amacrine cells stratifying in the OFF sublamina show changes in their lamination patterns prior to those stratifying in the ON sublamina. Amacrine cell plexes in the IPL were somewhat reduced by PNM9.5, particularly the OFF sublamina that contains the processes of OFF starburst and type-1 dopaminergic amacrine cells. AII amacrine cells are a key cell type in the primary rod circuit, and have been reported to remodel roughly concurrently with rod loss in the *rd10* retina, as evidenced by a reduction in immunoreactivity for Disabled-1 in AII amacrine cell processes by P40 (Barhoum et al., 2008). At advanced stages of photoreceptor loss, we found synapsin 1, VAMP-2 and SV2 immunoreactivity in discrete puncta in the INL and GCL. Processes containing these putative, ectopic synapses are likely to arise from amacrine cells, as the expression of synapsin 1 and the absence of VGluT1 and syntaxin 3 in these processes argues strongly against a bipolar cell or photoreceptor origin. It is not clear whether these puncta represent mature, functional synapses, collections of presynaptic precursor vesicles, or aberrant trafficking of proteins (McAlister and Wells, 1981; Ahmari et al., 2000; Friedman et al., 2000). However, previous studies have shown ectopic synapse formation in mice with photoreceptor synaptic ribbon defects (Specht et al., 2007), a photoreceptor-specific calcium channel mutation (Bayley and Morgans, 2007), and as a consequence of normal aging (Terzibasi et al., 2009).

One limitation of immunohistochemical analyses is that co-localization at the level of confocal microscopy does not prove a physical association between proteins nor does the presence of specific proteins demonstrate that they are organized into functional complexes. In degenerative processes, proteins can be mis-expressed or trafficked inappropriately to novel locations within a cell. However, we have shown the appropriate co-localization of multiple synaptic proteins and the continued stratification of different cell types in the IPL. When considered in conjunction with the long term preservation of the dendritic and axonal structure of retinal ganglion cells (Mazzoni et al., 2008), it is reasonable to suggest that at least some of the normal, functional circuitry in the inner retina is maintained in *rd10* mice, even after photoreceptor degeneration is complete.

The *rd10* mouse is increasingly being used for research to develop novel therapeutic interventions for *RP* (Otani et al., 2004; Boatright et al., 2006; Komeima et al., 2007; Corrochano et al., 2008; Pang et al., 2008; Phillips et al., 2008; Usui et al., 2009). Current strategies for stem-cell based therapies and retinal prosthetics to treat *RP* rely on the assumption that the remaining retinal circuitry remains intact. The preservation of the laminar organization and appropriate patterns of synaptic protein expression in the inner retina of the *rd10* mouse, even at late stages of the disease, lends both hope and direction for development of future treatments. However, early intervention will be a key factor for preventing the secondary remodeling of the surviving retina. One interesting possibility is that early transplantation of differentiated photoreceptors (MacLaren et al., 2006; West et al., 2008) or retinal stem cells (Tropepe et al., 2000; Ooto et al., 2004; MacLaren and Pearson, 2007; MacNeil et al., 2007; Bull et al., 2008; Klassen et al., 2008; Ohta et al., 2008) could delay or even prevent remodeling of the second order neurons and cell death by providing synaptic input to those circuits. Likewise, pharmacological replacement of lost glutamate release from photoreceptors might retard the severe negative remodeling of horizontal and bipolar cell processes and loss of key post-synaptic proteins such as

glutamate receptors. Such strategies could improve the chances of successful restoration of synaptic circuits between transplanted photoreceptors or stem cells and second-order neurons in the host retina. Late stage interventions will need to circumvent the consequences of both gliosis and the remodeling that occurs in second order neurons. Early intervention will also be key for retinal prosthetic approaches (Jensen and Rizzo, 2006; Pardue et al., 2006; Besch et al., 2008; Pardue et al., 2008; Butterwick et al., 2009), in order to take advantage of the high degree of preservation of retinal circuits at the level of the inner retina which our data and others (Mazzoni et al., 2008) suggest remains largely intact in the retinas of the *rd10* mouse model of *RP*, even following extended photoreceptor degeneration.

Supplementary Material

Refer to Web version on PubMed Central for supplementary material.

Acknowledgments

The authors thank Drs. Robert Margolskee and Kathleen Buckley for their generous gifts of antibodies and Dr. Machelle Pardue for the gift of mutant mouse eyes. Some of the results have previously been published in abstract form. Phillips J, Otteson DC, Sherry DM (2007) Invest. Ophthalmol. Vis. Sci. Abstr. 48: ARVO E-Abstract 4506.

Grant sponsors: Grant Sponsor: NIH, T32 EY07024 Houston Area Training Grant Predoctoral Fellowship (MJP), P30 EY07751-CORE (UHCO); Grant Sponsor: American Optometric Foundation Ezell Fellowship (MJP); Grant Sponsor: University of Houston College of Optometry: Vision Research Support Grant (MJP), Unrestricted funds (DCO); Grant Sponsor: OCAST HR08-149S (DMS); Grant Sponsor: University of Oklahoma Health Sciences Center (DMS).

Literature Cited

Ahmari SE, Buchanan J, Smith SJ. Assembly of presynaptic active zones from cytoplasmic transport packets. Nat Neurosci. 2000; 3:445–451. [PubMed: 10769383]

Airaksinen MS, Eilers J, Garaschuk O, Thoenen H, Konnerth A, Meyer M. Ataxia and altered dendritic calcium signaling in mice carrying a targeted null mutation of the calbindin D28k gene. Proc Natl Acad Sci U S A. 1997; 94:1488–1493. [PubMed: 9037080]

Banin E, Cideciyan AV, Alemán TS, Petters RM, Wong F, Milam AH, Jacobson SG. Retinal rod photoreceptor-specific gene mutation perturbs cone pathway development. Neuron. 1999; 23:549–557. [PubMed: 10433266]

Barhoum R, Martínez-Navarrete G, Corrochano S, Germain F, Fernandez-Sanchez L, de la Rosa EJ, de la Villa P, Cuenca N. Functional and structural modifications during retinal degeneration in the rd10 mouse. Neuroscience. 2008; 155:698–713. [PubMed: 18639614]

Bayley PR, Morgans CW. Rod bipolar cells and horizontal cells form displaced synaptic contacts with rods in the outer nuclear layer of the nob2 retina. J Comp Neurol. 2007; 500:286–298. [PubMed: 17111373]

Belichenko PV, Kleschevnikov AM, Masliah E, Wu C, Takimoto-Kimura R, Salehi A, Mobley WC. Excitatory-inhibitory relationship in the fascia dentata in the Ts65Dn mouse model of Down syndrome. J Comp Neurol. 2009; 512:453–466. [PubMed: 19034952]

Bellocchio EE, Hu H, Pohorille A, Chan J, Pickel VM, Edwards RH. The localization of the brain-specific inorganic phosphate transporter suggests a specific presynaptic role in glutamatergic transmission. J Neurosci. 1998; 18:8648–8659. [PubMed: 9786972]

Besch D, Sachs H, Szurman P, Gülicher D, Wilke R, Reinert S, Zrenner E, Bartz-Schmidt KU, Gekeler F. Extraocular surgery for implantation of an active subretinal visual prosthesis with external connections: feasibility and outcome in seven patients. Br J Ophthalmol. 2008; 92:1361–1368. [PubMed: 18662916]

Blanks JC, Adinolfi AM, Lolley RN. Synaptogenesis in the photoreceptor terminal of the mouse retina. J Comp Neurol. 1974; 156:81–93. [PubMed: 4836656]

Boatright JH, Moring AG, McElroy C, Phillips MJ, Do VT, Chang B, Hawes NL, Boyd AP, Sidney SS, Stewart RE, Minear SC, Chaudhury R, Ciavatta VT, Rodrigues CM, Steer CJ, Nickerson JM,

Pardue MT. Tool from ancient pharmacopoeia prevents vision loss. Mol Vis. 2006; 12:1706–1714. [PubMed: 17213800]

Bowes C, Li T, Danciger M, Baxter LC, Applebury ML, Farber DB. Retinal degeneration in the rd mouse is caused by a defect in the beta subunit of rod cGMP-phosphodiesterase. Nature. 1990; 347:677–680. [PubMed: 1977087]

Buckley K, Kelly RB. Identification of a transmembrane glycoprotein specific for secretory vesicles of neural and endocrine cells. J Cell Biol. 1985; 100:1284–1294. [PubMed: 2579958]

Bull ND, Limb GA, Martin KR. Human Müller stem cell (MIO-M1) transplantation in a rat model of glaucoma: survival, differentiation, and integration. Invest Ophthalmol Vis Sci. 2008; 49:3449–3456. [PubMed: 18408183]

Butterwick A, Huie P, Jones BW, Marc RE, Marmor M, Palanker D. Effect of shape and coating of a subretinal prosthesis on its integration with the retina. Exp Eye Res. 2009; 88:22–29. [PubMed: 18955050]

Carter-Dawson LD, LaVail MM, Sidman RL. Differential effect of the rd mutation on rods and cones in the mouse retina. Invest Ophthalmol Vis Sci. 1978; 17:489–498. [PubMed: 659071]

Celio MR, Baier W, Schärer L, Gregersen HJ, de Viragh PA, Norman AW. Monoclonal antibodies directed against the calcium binding protein Calbindin D-28k. Cell Calcium. 1990; 11:599–602. [PubMed: 2285928]

Chang B, Hawes NL, Pardue MT, German AM, Hurd RE, Davisson MT, Nusinowitz S, Rengarajan K, Boyd AP, Sidney SS, Phillips MJ, Stewart RE, Chaudhury R, Nickerson JM, Heckenlively JR, Boatright JH. Two mouse retinal degenerations caused by missense mutations in the beta-subunit of rod cGMP phosphodiesterase gene. Vision Res. 2007; 47:624–633. [PubMed: 17267005]

Chua J, Fletcher EL, Kalloniatis M. Functional remodeling of glutamate receptors by inner retinal neurons occurs from an early stage of retinal degeneration. J Comp Neurol. 2009; 514:473–491. [PubMed: 19350664]

Corrochano S, Barhoum R, Boya P, Arroba AI, Rodríguez-Muela N, Gómez-Vicente V, Bosch F, de Pablo F, de la Villa P, de la Rosa EJ. Attenuation of vision loss and delay in apoptosis of photoreceptors induced by proinsulin in a mouse model of retinitis pigmentosa. Invest Ophthalmol Vis Sci. 2008; 49:4188–4194. [PubMed: 18515565]

Cuenca N, Pinilla I, Sauvé Y, Lund R. Early changes in synaptic connectivity following progressive photoreceptor degeneration in RCS rats. Eur J Neurosci. 2005; 22:1057–1072. [PubMed: 16176347]

Daiger SP, Bowne SJ, Sullivan LS. Perspective on genes and mutations causing retinitis pigmentosa. Arch Ophthalmol. 2007; 125:151–158. [PubMed: 17296890]

Eliasieh K, Liets LC, Chalupa LM. Cellular reorganization in the human retina during normal aging. Invest Ophthalmol Vis Sci. 2007; 48:2824–2830. [PubMed: 17525218]

Fisher LJ. Development of synaptic arrays in the inner plexiform layer of neonatal mouse retina. J Comp Neurol. 1979; 187:359–372. [PubMed: 489784]

Fisher SK, Lewis GP, Linberg KA, Verardo MR. Cellular remodeling in mammalian retina: results from studies of experimental retinal detachment. Prog Retin Eye Res. 2005; 24:395–431. [PubMed: 15708835]

Friedman HV, Bresler T, Garner CC, Ziv NE. Assembly of new individual excitatory synapses: time course and temporal order of synaptic molecule recruitment. Neuron. 2000; 27:57–69. [PubMed: 10939331]

Garbelli R, Inverardi F, Medici V, Amadeo A, Verderio C, Matteoli M, Frassoni C. Heterogeneous expression of SNAP-25 in rat and human brain. J Comp Neurol. 2008; 506:373–386. [PubMed: 18041776]

Gargini C, Terzibasi E, Mazzoni F, Strettoi E. Retinal organization in the retinal degeneration 10 (rd10) mutant mouse: a morphological and ERG study. J Comp Neurol. 2007; 500:222–238. [PubMed: 17111372]

Ghosh KK, Bujan S, Haverkamp S, Feigenspan A, Wässle H. Types of bipolar cells in the mouse retina. J Comp Neurol. 2004; 469:70–82. [PubMed: 14689473]

Greenlee MH, Roosevelt CB, Sakaguchi DS. Differential localization of SNARE complex proteins SNAP-25, syntaxin, and VAMP during development of the mammalian retina. J Comp Neurol. 2001; 430:306–320. [PubMed: 11169469]

Hartong DT, Berson EL, Dryja TP. Retinitis pigmentosa. Lancet. 2006; 368:1795–1809. [PubMed: 17113430]

Haverkamp S, Wässle H. Immunocytochemical analysis of the mouse retina. J Comp Neurol. 2000; 424:1–23. [PubMed: 10888735]

Haverkamp S, Wässle H. Characterization of an amacrine cell type of the mammalian retina immunoreactive for vesicular glutamate transporter 3. J Comp Neurol. 2004; 468:251–263. [PubMed: 14648683]

Hepp R, Langley K. SNAREs during development. Cell Tissue Res. 2001; 305:247–253. [PubMed: 11545262]

Huang L, Max M, Margolskee RF, Su H, Masland RH, Euler T. G protein subunit G gamma 13 is coexpressed with G alpha o, G beta 3, and G beta 4 in retinal ON bipolar cells. J Comp Neurol. 2003; 455:1–10. [PubMed: 12454992]

Huang L, Shanker YG, Dubauskaite J, Zheng JZ, Yan W, Rosenzweig S, Spielman AI, Max M, Margolskee RF. Ggamma13 colocalizes with gustducin in taste receptor cells and mediates IP3 responses to bitter denatonium. Nat Neurosci. 1999; 2:1055–1062. [PubMed: 10570481]

Jensen RJ, Rizzo JF 3rd. Thresholds for activation of rabbit retinal ganglion cells with a subretinal electrode. Exp Eye Res. 2006; 83:367–373. [PubMed: 16616739]

Johnson J, Sherry DM, Liu X, Fremeau RT Jr, Seal RP, Edwards RH, Copenhagen DR. Vesicular glutamate transporter 3 expression identifies glutamatergic amacrine cells in the rodent retina. J Comp Neurol. 2004; 477:386–398. [PubMed: 15329888]

Johnson PT, Brown MN, Pulliam BC, Anderson DH, Johnson LV. Synaptic pathology, altered gene expression, and degeneration in photoreceptors impacted by drusen. Invest Ophthalmol Vis Sci. 2005; 46:4788–4795. [PubMed: 16303980]

Jones BW, Marc RE. Retinal remodeling during retinal degeneration. Exp Eye Res. 2005; 81:123–137. [PubMed: 15916760]

Keeler CE. The inheritance of a retinal abnormality in white mice. Proc Natl Acad Sci U S A. 1924; 10:329–333. [PubMed: 16576828]

Kerr DS, Von Dannecker LE, Davalos M, Michaloski JS, Malnic B. Ric-8B interacts with G alpha olf and G gamma 13 and co-localizes with G alpha olf, G beta 1 and G gamma 13 in the cilia of olfactory sensory neurons. Mol Cell Neurosci. 2008; 38:341–348. [PubMed: 18462949]

Klassen H, Warfvinge K, Schwartz PH, Kiilgaard JF, Shamie N, Jiang C, Samuel M, Scherfig E, Prather RS, Young MJ. Isolation of progenitor cells from GFP-transgenic pigs and transplantation to the retina of allorecipients. Cloning Stem Cells. 2008; 10:391–402. [PubMed: 18729769]

Komeima K, Rogers BS, Campochiaro PA. Antioxidants slow photoreceptor cell death in mouse models of retinitis pigmentosa. J Cell Physiol. 2007; 213:809–815. [PubMed: 17520694]

Liets LC, Eliasieh K, van der List DA, Chalupa LM. Dendrites of rod bipolar cells sprout in normal aging retina. Proc Natl Acad Sci U S A. 2006; 103:12156–12160. [PubMed: 16880381]

Lynch BA, Lambeng N, Nocka K, Kensel-Hammes P, Bajjalieh SM, Matagne A, Fuks B. The synaptic vesicle protein SV2A is the binding site for the antiepileptic drug levetiracetam. Proc Natl Acad Sci U S A. 2004; 101:9861–9866. [PubMed: 15210974]

MacLaren RE, Pearson RA. Stem cell therapy and the retina. Eye. 2007; 21:1352–1359. [PubMed: 17914439]

MacLaren RE, Pearson RA, MacNeil A, Douglas RH, Salt TE, Akimoto M, Swaroop A, Sowden JC, Ali RR. Retinal repair by transplantation of photoreceptor precursors. Nature. 2006; 444:203–207. [PubMed: 17093405]

MacNeil A, Pearson RA, MacLaren RE, Smith AJ, Sowden JC, Ali RR. Comparative analysis of progenitor cells isolated from the iris, pars plana, and ciliary body of the adult porcine eye. Stem Cells. 2007; 25:2430–2438. [PubMed: 17600111]

Marc RE, Jones BW. Retinal remodeling in inherited photoreceptor degenerations. Mol Neurobiol. 2003; 28:139–147. [PubMed: 14576452]

Marc RE, Jones BW, Anderson JR, Kinard K, Marshak DW, Wilson JH, Wensel T, Lucas RJ. Neural reprogramming in retinal degeneration. Invest Ophthalmol Vis Sci. 2007; 48:3364–3371. [PubMed: 17591910]

Marc RE, Jones BW, Watt CB, Strettoi E. Neural remodeling in retinal degeneration. Prog Retin Eye Res. 2003; 22:607–655. [PubMed: 12892644]

Marc RE, Jones BW, Watt CB, Vazquez-Chona F, Vaughan DK, Organisciak DT. Extreme retinal remodeling triggered by light damage: implications for age related macular degeneration. Mol Vis. 2008; 14:782–806. [PubMed: 18483561]

Martínez A, Alcántara S, Borrell V, Del Río JA, Blasi J, Otal R, Campos N, Boronat A, Barbacid M, Silos-Santiago I, Soriano E. TrkB and TrkC signaling are required for maturation and synaptogenesis of hippocampal connections. J Neurosci. 1998; 18:7336–7350. [PubMed: 9736654]

Mazzoni F, Novelli E, Strettoi E. Retinal ganglion cells survive and maintain normal dendritic morphology in a mouse model of inherited photoreceptor degeneration. J Neurosci. 2008; 28:14282–14292. [PubMed: 19109509]

McAllister JP, Wells J. The structural organization of the ventral posterolateral nucleus in the rat. J Comp Neurol. 1981; 197:271–301. [PubMed: 7276236]

Melone M, Burette A, Weinberg RJ. Light microscopic identification and immunocytochemical characterization of glutamatergic synapses in brain sections. J Comp Neurol. 2005; 492:495–509. [PubMed: 16228991]

Montana V, Ni Y, Sunjara V, Hua X, Parpura V. Vesicular glutamate transporter-dependent glutamate release from astrocytes. J Neurosci. 2004; 24:2633–2642. [PubMed: 15028755]

Morgan JE, Datta AV, Erichsen JT, Albon J, Boulton ME. Retinal ganglion cell remodelling in experimental glaucoma. Adv Exp Med Biol. 2006; 572:397–402. [PubMed: 17249602]

Ohta K, Ito A, Tanaka H. Neuronal stem/progenitor cells in the vertebrate eye. Dev Growth Differ. 2008; 50:253–259. [PubMed: 18336580]

Ooto S, Akagi T, Kageyama R, Akita J, Mandai M, Honda Y, Takahashi M. Potential for neural regeneration after neurotoxic injury in the adult mammalian retina. Proc Natl Acad Sci U S A. 2004; 101:13654–13659. [PubMed: 15353594]

Otani A, Dorrell MI, Kinder K, Moreno SK, Nusinowitz S, Banin E, Heckenlively J, Friedlander M. Rescue of retinal degeneration by intravitreally injected adult bone marrow-derived lineage-negative hematopoietic stem cells. J Clin Invest. 2004; 114:765–774. [PubMed: 15372100]

Pang JJ, Boye SL, Kumar A, Dinculescu A, Deng W, Li J, Li Q, Rani A, Foster TC, Chang B, Hawes NL, Boatright JH, Hauswirth WW. AAV-mediated gene therapy for retinal degeneration in the rd10 mouse containing a recessive PDEbeta mutation. Invest Ophthalmol Vis Sci. 2008; 49:4278–4283. [PubMed: 18586879]

Pardue MT, Ball SL, Phillips MJ, Faulkner AE, Walker TA, Chow AY, Peachey NS. Status of the feline retina 5 years after subretinal implantation. J Rehabil Res Dev. 2006; 43:723–732. [PubMed: 17310421]

Pardue MT, Walker TA, Faulkner AE, Kim MK, Bonner CM, McLean GY. Implantation of mouse eyes with a subretinal microphotodiode array. Adv Exp Med Biol. 2008; 613:377–382. [PubMed: 18188967]

Peichl L, González-Soriano J. Morphological types of horizontal cell in rodent retinae: a comparison of rat, mouse, gerbil, and guinea pig. Vis Neurosci. 1994; 11:501–517. [PubMed: 8038125]

Phillips MJ, Walker TA, Choi HY, Faulkner AE, Kim MK, Sidney SS, Boyd AP, Nickerson JM, Boatright JH, Pardue MT. Tauroursodeoxycholic acid preservation of photoreceptor structure and function in the rd10 mouse through postnatal day 30. Invest Ophthalmol Vis Sci. 2008; 49:2148–2155. [PubMed: 18436848]

Pittler SJ, Keeler CE, Sidman RL, Baehr W. PCR analysis of DNA from 70-year-old sections of rodless retina demonstrates identity with the mouse rd defect. Proc Natl Acad Sci U S A. 1993; 90:9616–9619. [PubMed: 8415750]

Puthussery T, Gayet-Primo J, Pandey S, Duvoisin RM, Taylor WR. Differential loss and preservation of glutamate receptor function in bipolar cells in the rd10 mouse model of retinitis pigmentosa. Eur J Neurosci. 2009; 29:1533–1542. [PubMed: 19385989]

Schoch S, Deák F, Königstorfer A, Mozhayeva M, Sara Y, Südhof TC, Kavalali ET. SNARE function analyzed in synaptobrevin/VAMP knockout mice. Science. 2001; 294:1117–1122. [PubMed: 11691998]

Sherry DM, Mitchell R, Standifer KM, du Plessis B. Distribution of plasma membrane-associated syntaxins 1 through 4 indicates distinct trafficking functions in the synaptic layers of the mouse retina. BMC Neurosci. 2006; 7:54. [PubMed: 16839421]

Sherry DM, Wang MM, Bates J, Frishman LJ. Expression of vesicular glutamate transporter 1 in the mouse retina reveals temporal ordering in development of rod vs. cone and ON vs. OFF circuits. J Comp Neurol. 2003a; 465:480–498. [PubMed: 12975811]

Sherry DM, Wang MM, Frishman LJ. Differential distribution of vesicle associated membrane protein isoforms in the mouse retina. Mol Vis. 2003b; 9:673–688. [PubMed: 14685145]

Sohocki MM, Daiger SP, Bowne SJ, Rodriquez JA, Northrup H, Heckenlively JR, Birch DG, Mintz-Hittner H, Ruiz RS, Lewis RA, Saperstein DA, Sullivan LS. Prevalence of mutations causing retinitis pigmentosa and other inherited retinopathies. Hum Mutat. 2001; 17:42–51. [PubMed: 11139241]

Specht D, Tom Dieck S, Ammermüller J, Regus-Leidig H, Gundelfinger ED, Brandstätter JH. Structural and functional remodeling in the retina of a mouse with a photoreceptor synaptopathy: plasticity in the rod and degeneration in the cone system. Eur J Neurosci. 2007; 26:2506–2515. [PubMed: 17970721]

Strettoi E, Pignatelli V. Modifications of retinal neurons in a mouse model of retinitis pigmentosa. Proc Natl Acad Sci U S A. 2000; 97:11020–11025. [PubMed: 10995468]

Strettoi E, Pignatelli V, Rossi C, Porciatti V, Falsini B. Remodeling of second-order neurons in the retina of rd/rd mutant mice. Vision Res. 2003; 43:867–877. [PubMed: 12668056]

Terzibasi E, Calamusa M, Novelli E, Domenici L, Strettoi E, Cellerino A. Age-dependent remodelling of retinal circuitry. Neurobiol Aging. 2009; 30:819–828. [PubMed: 17920161]

Tropepe V, Coles BL, Chiasson BJ, Horsford DJ, Elia AJ, McInnes RR, van der Kooy D. Retinal stem cells in the adult mammalian eye. Science. 2000; 287:2032–2036. [PubMed: 10720333]

Usui S, Komeima K, Lee SY, Jo YJ, Ueno S, Rogers BS, Wu Z, Shen J, Lu L, Oveson BC, Rabinovitch PS, Campochiaro PA. Increased expression of catalase and superoxide dismutase 2 reduces cone cell death in retinitis pigmentosa. Mol Ther. 2009; 17:778–786. [PubMed: 19293779]

Wang MM, Janz R, Belizaire R, Frishman LJ, Sherry DM. Differential distribution and developmental expression of synaptic vesicle protein 2 isoforms in the mouse retina. J Comp Neurol. 2003; 460:106–122. [PubMed: 12687700]

Wenthold RJ, Yokotani N, Doi K, Wada K. Immunochemical characterization of the non-NMDA glutamate receptor using subunit-specific antibodies. Evidence for a hetero-oligomeric structure in rat brain. J Biol Chem. 1992; 267:501–507. [PubMed: 1309749]

West EL, Pearson RA, Tschernutter M, Sowden JC, MacLaren RE, Ali RR. Pharmacological disruption of the outer limiting membrane leads to increased retinal integration of transplanted photoreceptor precursors. Exp Eye Res. 2008; 86:601–611. [PubMed: 18294631]

Winsky L, Nakata H, Martin BM, Jacobowitz DM. Isolation, partial amino acid sequence, and immunohistochemical localization of a brain-specific calcium-binding protein. Proc Natl Acad Sci U S A. 1989; 86:10139–10143. [PubMed: 2602362]

Young RW. Cell differentiation in the retina of the mouse. Anat Rec. 1985; 212:199–205. [PubMed: 3842042]

Zhang J, Yang Z, Wu SM. Development of cholinergic amacrine cells is visual activity-dependent in the postnatal mouse retina. J Comp Neurol. 2005; 484:331–343. [PubMed: 15739235]

Zhou Q, Xiao J, Liu Y. Participation of syntaxin 1A in membrane trafficking involving neurite elongation and membrane expansion. J Neurosci Res. 2000; 61:321–328. [PubMed: 10900079]

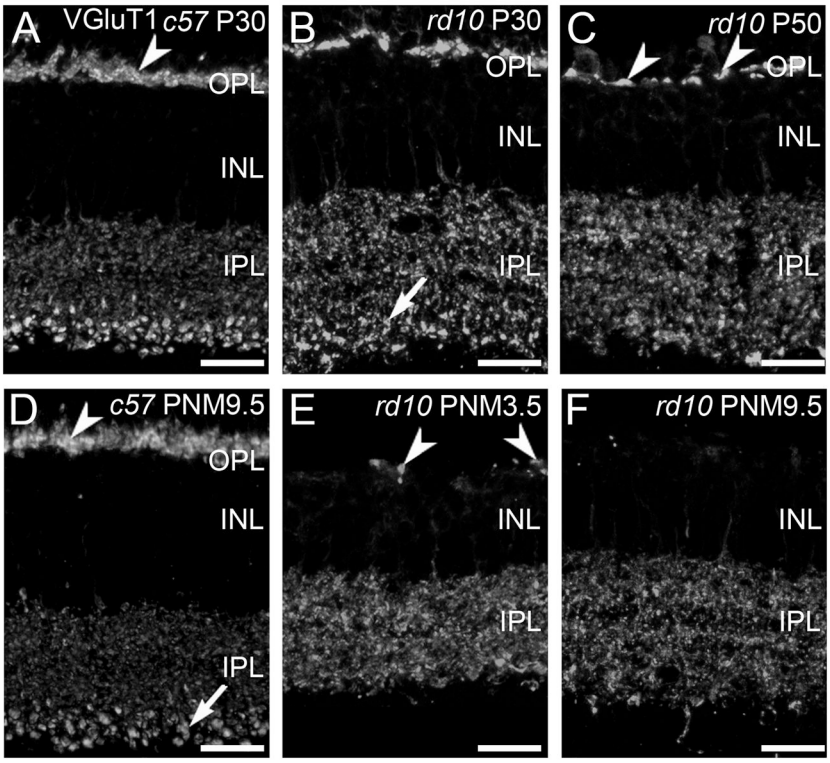

Figure 1. VGluT1 expression in *C57BL/6* and *rd10* retina

A, D: In the retinas from wild-type *C57BL/6* (*c57*) mice at postnatal day 30 (P30, panel A) and postnatal month 9.5 (PNM9.5, panel D), VGluT1 antibodies label rod and cone terminals in the outer plexiform layer (OPL) (arrowhead) and bipolar cell terminals in the inner plexiform layer (IPL). Large, lobular rod bipolar cell terminals in the innermost IPL are prominently labeled (arrow). **B, C, E, F:** VGluT1 expression in the *rd10* retina from P30 to PNM9.5. **B.** At P30, prominent gaps between VGluT1-positive photoreceptor terminals are present in OPL. Rod bipolar cell terminals in the IPL (arrow) are less distinctive than in the wild-type retina. **C.** At P50, VGluT1 staining in the OPL is reduced (arrowheads). The spacing and morphology of labeled terminals indicates that primarily cone pedicles remain at this time point. **E.** At PNM3.5, VGluT1 staining in the *rd10* OPL labels the few surviving cone terminals (arrowheads). In the IPL, no morphologically distinct rod bipolar cell terminals are discernable. **F.** At PNM9.5, little to no expression of VGluT1 is detected in the OPL; VGluT1 is still present in the IPL. Scale bar = 20 μm, all panels.

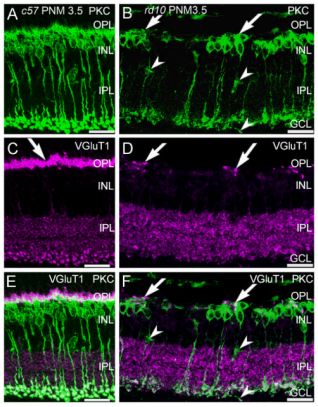

Figure 2. PKCα and VGluT1 double labeling of *C57BL/6* and *rd10* retinas

A, C, E: *C57BL/6* (*c57*) retina at PNM3.5. **A**. Rod bipolar cells labeled with antibodies against protein kinase C-α (PKC) show normal morphology. **C.** VGluT1 labels photoreceptor terminals in the OPL (arrow) and bipolar cell terminals in the IPL. **E.** Merged image of PKC and VGluT1 labeling. PKC-positive rod bipolar cell dendrites extend into the plexus of VGluT1-positive photoreceptor terminals in the OPL. Rod bipolar cell terminals in the IPL show strong labeling for VGluT1. **B, D, F:** *rd10* retina at PNM3.5. **B.** In the *rd10* retina, rod bipolar cells have retracted their dendrites and have disorganized axon terminals, with some ectopic processes (arrowheads). Surviving rod bipolar cell bodies are found in clusters (arrows). **D.** Scattered VGluT1-positive cone terminals remain in the OPL at PNM3.5. **F.** Merged image of PKC and VGluT1 labeling. Rod bipolar cell bodies cluster near the remaining VGluT1-positive cone terminals in the OPL (arrows). Rod bipolar cell terminals in the inner IPL show reduced labeling for VGluT1, with ectopic processes lacking VGluT1 staining (arrowheads). Scale bar = 20 μm, all panels.

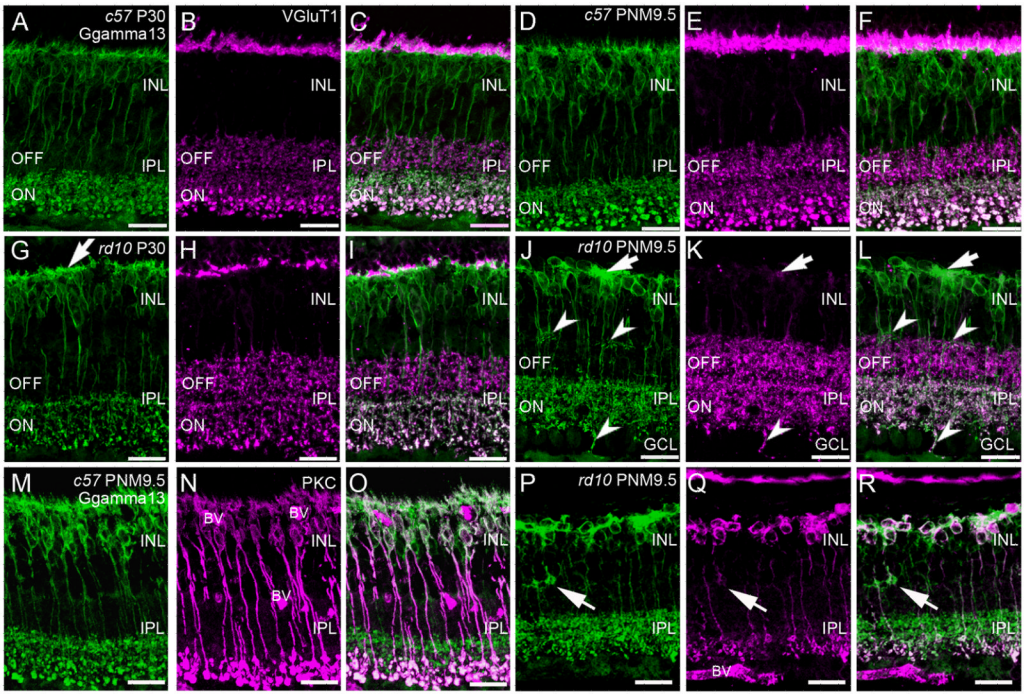

Figure 3. Immunostaining of ON-cone and rod bipolar cells in *C57BL/6* and *rd10* retinas

A–C: *C57BL/6* (*c57*) retina at P30. **A.** Gγ13 labeling of dendrites, cell bodies and axon terminals of all ON-bipolar cells (rod and cone). Large, lobular rod bipolar cell terminals in the innermost IPL are intensely labeled. **B.** Antibodies against vesicular glutamate transporter 1 (VGluT1) label the axon terminals of rod and cone photoreceptors in the OPL and both ON and OFF bipolar cells in the IPL. **C.** Overlay of panels A and B showing ON-OFF stratification in the IPL. Terminals of OFF-cone bipolar cells in the distal IPL are VGluT1-positive, Gγ13-negative. Terminals of ON-cone and rod bipolar cells are VGluT1-positive and Gγ13-positive and can be distinguished by size and position in the inner IPL. **D–F:** *C57BL/6* retina at PNM9.5. The labeling patterns for Gγ13 (**D**) and VGluT1 (**E**) remains unchanged. **F.** Overlay of D and E. **G–I:** *rd10* retina at P30. **G.** Labeling for Gγ13 shows abnormally thickened dendritic processes in the OPL (arrow). ON bipolar cell terminals stratify in the correct sublamina of the innermost IPL. **H.** A discontinuous band of VGluT1 immunoreactivity is still present in OPL. VGluT1-positive bipolar cell terminals are present throughout the IPL but the rod bipolar terminals are less distinctive than in the wild-type retina. **I.** Overlay of Gγ13 and VGluT1 labeling shows proper lamination of ON and OFF bipolar cell terminals in the IPL. **J–L:** *rd10* retina at PNM9.5. **J.** Gγ13-positive dendritic processes are generally absent, although some dense areas of staining persist (arrow). Most ON bipolar cell terminals stratify properly within the ON sublamina of the IPL, although some ectopic processes are present at the INL/IPL border and extend into the ganglion cell layer (GCL) (arrowheads). **K.** Few sites of VGluT1 labeling remain in the OPL (arrow). Bipolar cell terminals throughout the IPL show VGluT1 labeling but rod bipolar cell terminals are not morphologically identifiable. **L.** Overlay of Gγ13 and VGluT1 labeling. In the OPL, areas of dense Gγ13 staining are associated with remaining VGluT1-positive puncta (arrow). In the IPL, Gγ13 and VGluT1 co-localize in ON bipolar cell terminals and the ON and OFF stratification remains largely intact. Many ectopic Gγ13-positive processes (arrowheads) also show VGluT1 labeling. **M–O:** Retinas from *C57BL/6* at PNM9.5 immunostained for **(M)** Gγ13, showing all ON bipolar cells and **(N)** PKC, showing rod bipolar cells. **O.** An overlay of M and N distinguishes rod and ON cone bipolar cells. **P–R:** Retinas from *rd10* mice at PNM9.5 immunostained for **(P)** Gγ13, and **(Q)** PKC.

Ectopic processes in the INL show strong Gγ13 labeling and faint PKC labeling (arrows). **R.** Overlay of P and Q showing clusters of rod and ON-cone bipolar cells in the INL. The appropriate stratification of rod bipolar and ON-cone bipolar cell terminals in the IPL is still apparent. Scale bar = 20 μm, all panels.

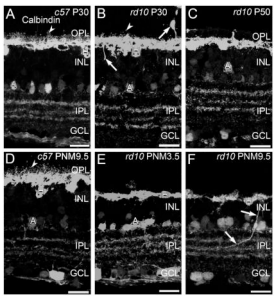

Figure 4. Calbindin immunostaining in *C57BL/6* and *rd10* retinas

A, D: *C57BL/6* (*c57*) retina at P30 (A) and PNM9.5 (D). Antibodies against calbindin label horizontal cells and their fine processes associated with the terminals of photoreceptors (arrowheads) in the OPL and a subset of amacrine cells and their terminals in the INL and IPL. **B, C, E, F:** *rd10* mouse retina. **B.** At P30, during early stages of degeneration, puncta associated with horizontal cell dendrites and axon terminals are reduced but still present (arrowhead). Some horizontal cells sprout ectopic processes (arrows). **C.** At P50, the puncta associated with fine processes of horizontal cells are no longer detected. **E.** At PNM3.5, staining of horizontal cell lateral processes in OPL is greatly reduced. **F.** At PNM9.5, gaps are visible in the calbindin-positive horizontal cell plexus in the OPL. Ectopic processes from horizontal cells are still detected (arrows). Amacrine cells show minimal changes and the stratified organization of amacrine cell processes in the IPL is preserved. Scale bar = 20 μm, all panels.

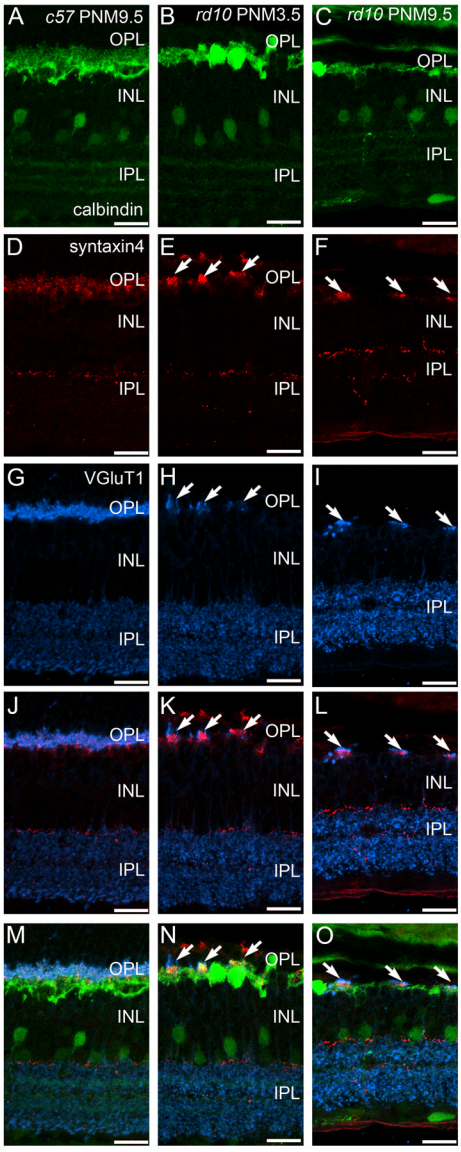

Figure 5. Immunostaining for calbindin, syntaxin 4 and VGluT1 in the *C57BL/6* and *rd10* retinas at late stages of degeneration

A, D, G, J, M: *C57BL/6* (*c57*) retina at PNM9.5. **A**. Calbindin labeling. **D.** Syntaxin 4 labeling of the fine dendrites of horizontal cells and a sparse plexus in the IPL. **G.** VGluT1 labeling. **J.** Overlay of panels D and G showing the direct apposition of presynaptic VGluT1 expression with postsynaptic syntaxin 4 expression in the OPL. **M.** Overlay of panels A, D, and G showing the normal relationship of presynaptic VGluT1 and syntaxin 4 in fine horizontal cell processes and the remainder of the horizontal cell plexus in the OPL. **B, E, H, K, N:** *rd10* retina at PNM3.5. **B.** Calbindin labeling reveals horizontal cell process loss. **E.** Syntaxin 4 labeling in the OPL is restricted to small, widely spaced patches (arrows), but remains essentially normal in the IPL. **H.** Restricted sites of VGluT1 labeling in the OPL (arrows). **K.** Overlay of panels E and H showing direct apposition of syntaxin 4 and VGluT1 labeling in the OPL. **N.** Overlay of panels B, E, and H, shows the relationship of presynaptic VGluT1, syntaxin 4 and the horizontal cell plexus in the OPL. **C, F, I, L, O:** *rd10* retina at PNM9.5. **C.** Calbindin labeling reveals a severe reduction of horizontal cell processes at PNM9.5. **F.** Patches of syntaxin 4 labeling in the OPL become smaller at PNM9.5 in the

rd10 retina (arrows). **I.** Surviving cone terminals in the PNM9.5 *rd10* OPL express VGluT1. **L.** Overlay of panels F and I showing juxtaposition of syntaxin 4 and VGluT1 labeling in the OPL. **O.** Overlay of panels C, F, and I, showing the close physical relationship between syntaxin 4 expression, the horizontal cell plexus and surviving terminals of cones in the OPL at late stages of degeneration. Scale bar = 20 μm, all panels.

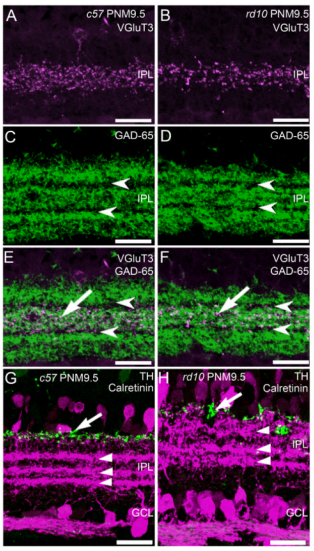

Figure 6. Stratification of amacrine cell processes in the plexiform layers of *C57BL/6* and *rd10* retinas at PNM9.5

A. *C57BL/6* (*c57*) retina immunostained with antibodies against the vesicular glutamate transporter 3 (VGluT3) reveals stratification of putative glutamatergic amacrine cells in the middle of the IPL. **B.** In the *rd10* retina, VGluT3-positive amacrine cells retain normal stratification in the middle of the IPL. **C.** In the *c57* retina, antibodies against the 65kDa isoform of glutamic acid decarboxylase (GAD-65) label 3 distinct strata containing the terminals of GABAergic amacrine cells. Arrowheads indicate the location of the GAD-65-negative processes of starburst amacrine cells. **D.** In the *rd10* retina, the normal stratification of GAD-65-positive terminals in the IPL is present at PNM9.5. **E.** Overlay of VGluT3 (A) and GAD-65 (C) immunolabeling in the wild-type *c57* retina shows stratification of the VGluT3 amacrine cells in the IPL (arrow) between the GAD-65-negative, starburst amacrine cell strata (arrowheads). **F.** Overlay of VGluT3 (B) and GAD-65 (D) immunolabeling in the *rd10* retina showing the continued stratification of VGluT3 amacrine cell processes in the IPL at PNM9.5. **G.** Wild-type *c57* mouse retina at PNM9.5, immunostained with antibodies against tyrosine hydroxylase (TH, green), and calretinin (magenta). Antibodies against TH label dopaminergic amacrine cells and their processes along the INL/IPL border (arrow). Antibodies against calretinin labels amacrine cells and their processes and reveal three distinct strata in the IPL (arrowheads). The upper and lower strata correspond to the processes of the OFF and ON starburst amacrine cells, respectively. Calretinin labeling also is present in cells in the ganglion cell layer and ganglion cell axons. **H.** Double labeling for TH and calretinin in the *rd10* retina at PNM9.5. Despite some disorganization, the TH-positive processes of the dopaminergic amacrine cells are still located along the INL/IPL border (arrow). Three strata of calretinin-positive amacrine cell processes are still present in the IPL. However, the OFF starburst amacrine cell stratum appears more diffuse. Labeling of cells and axons in the GCL appears normal. Scale bars = 20 μm, all panels.

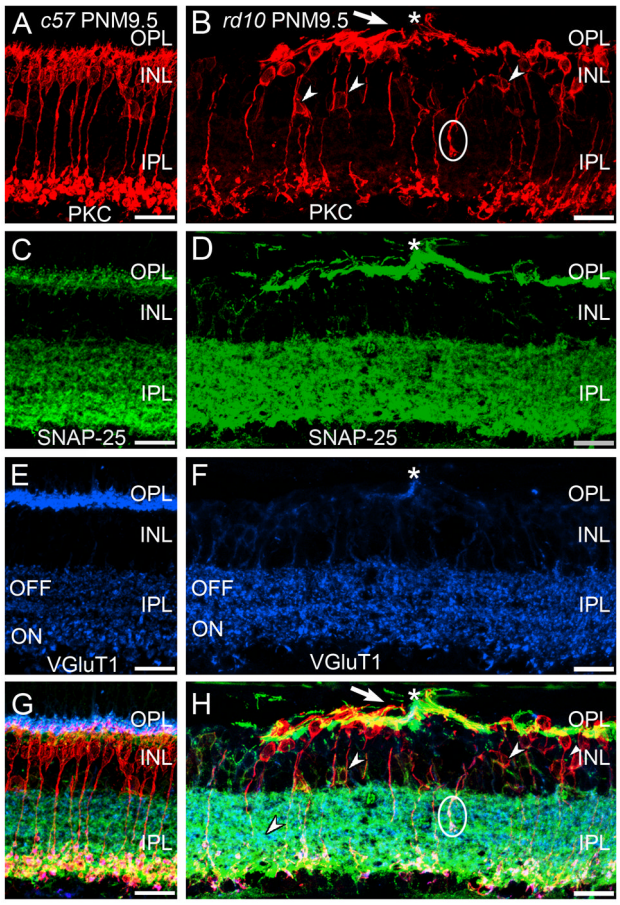

Figure 7. Immunostaining for PKC, SNAP-25 and VGluT1 in the *C57BL/6* and *rd10* retina

A, C, E, G: Wild-type *C57BL/6 (c57)* retina at PNM9.5. A. Antibodies against protein kinase C-α (PKC) identify rod bipolar cells, which show normal morphology and stratification in the IPL. **C.** In c*57* retina, the presynaptic SNARE protein SNAP-25 is found in the conventional and ribbon synapses of the OPL and IPL. **E.** VGluT1 expression in the *C57BL/6* retina. **G.** Overlay of panels A, C and E. **B, D, F, H:** *rd10* retina at PNM9.5. **B.** Although many rod bipolar cells are lost by PNM9.5 and most surviving rod bipolar cells have retracted their dendrites, rod bipolar cells located near surviving cone terminals extend abnormal, thickened dendrites (arrow) toward the surviving cone terminals (asterisk, see panel F). Many ectopic rod bipolar cell bodies (small arrowheads) and processes (circle) are present. Note the sparse plexus of rod bipolar cell terminals in the IPL. **D.** SNAP-25 labeling is highly elevated in the OPL but appears unchanged in the IPL. The cellular origin of the highly SNAP-25-positive processes in the outer retina is uncertain. **F.** A single VGluT1-positive terminal remains in this region of the OPL (asterisk). **H.** Overlay of panels B, D and F. Abnormal PKC-positive rod bipolar cell dendrites extend toward the surviving VGluT1-positive terminal (asterisk). Scale bar = 20 μm, all panels.

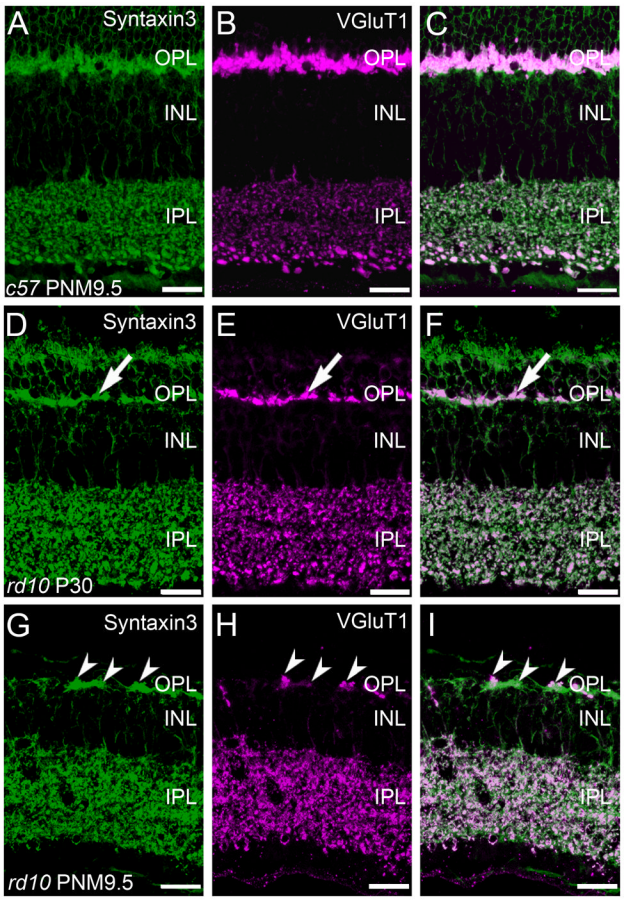

Figure 8.

Glutamate receptors are progressively lost from horizontal cells in the rd10 retina. A-C: GluR4 localizes to the tips of horizontal cell dendrites in the wildtype retina at PNM9.5. A. GluR4 receptor expression in the OPL in the wildtype C57BL/6 retina. B. Calbindin labeling in horizontal cells in the wildtype C57BL/6 retina. C. Overlay of GluR4 and calbindin labeling. GluR4 often localizes to the fine dendritic tips of horizontal cells. D-F: GluR4 localization in the rd10 OPL at PN50. D. GluR4 expression in the rd10 retina at PN50. At this age, GluR4 receptors are decreased in number and often appear in discreet clusters (arrows) that likely correspond to the location of cone terminals. E. The fine dendritic tips of horizontal cells have largely disappeared in the rd10 retina at PN50, but the thicker processes within the proximal OPL remain. F. Overlay of GluR4 and calbindin labeling. The clusters of remaining GluR4 receptors are localized to the same region of the OPL occupied by the thick processes of the horizontal cells. G-I: GluR4 localization in the rd10 OPL at PNM9.5. G.GluR4 expression is drastically reduced in the OPL of the rd10 retina at PNM9.5. The remaining GluR4 are found in small aggregates (arrow). H. Horizontal cell processes are dramatically reduced in the rd10 retina at PNM9.5. I. The remaining GluR4 expression corresponds to some of the remaining horizontal cell processes (arrow). Scale bar = 20 μm, all panels.

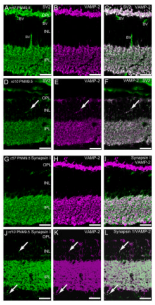

Figure 9.

Surviving photoreceptors promote local rod bipolar cell survival and remodeling of rod bipolar cell dendrites. A, C, E, G: Triple labeling for PKCα, SNAP-25 (a ubiquitous synaptic SNARE protein) and VGluT1 in the wildtype C57BL/6 retina at PNM9.5. A. PKCα expression identifies rod bipolar cells, which show normal morphology and stratification in the IPL. C. In the wildtype C57BL/6 retina, the presynaptic SNARE protein SNAP-25 is found in conventional and ribbon synapses in both plexiform layers. E. VGluT1 expression in the C57BL/6 retina. G. Overlay of labeling for PKCα, SNAP-25 and VGluT1 in the wildtype C57BL/6 retina. B, D, F, H: Triple labeling for PKCα, SNAP-25, and VGluT1 in the rd10 retina at PNM9.5. B. Although many rod bipolar cells are lost by PNM9.5 and most surviving rod bipolar cells have retracted their dendrites, those rod bipolar cells located near surviving cone terminals extend abnormal, thickened dendrites (arrow) toward the surviving cone terminals (asterisk, see panel F). Many ectopic cell bodies (arrowheads) and axon terminals are also present (circle). Note the sparse plexus of rod bipolar cell terminals in the IPL. D. SNAP-25 labeling appears normal in the IPL, but is highly elevated in the OPL of the rd10 retina at PNM9.5. F. A single surviving cone terminal expressing VGluT1 is present in this region of the OPL (asterisk). Labeling for VGlut1 is present in bipolar cell terminals in the ON and OFF sublaminae of the IPL. H. Overlay of labeling for PKCα, SNAP-25 and VGluT1 in the rd10 retina reveals abnormal rod bipolar cell dendrites extending toward the surviving cone terminal (asterisk). The cellular origin of the highly SNAP-25 positive processes in the outer retina is unclear. Given the dearth of photoreceptors at this late stage of degeneration, the labeling does not arise from photoreceptor terminals. Comparison of SNAP-25 and PKCα labeling indicates that elevated SNAP-25 is not associated specifically with the abnormal rod bipolar cell dendrites. Scale bar = 20 μm, all panels.

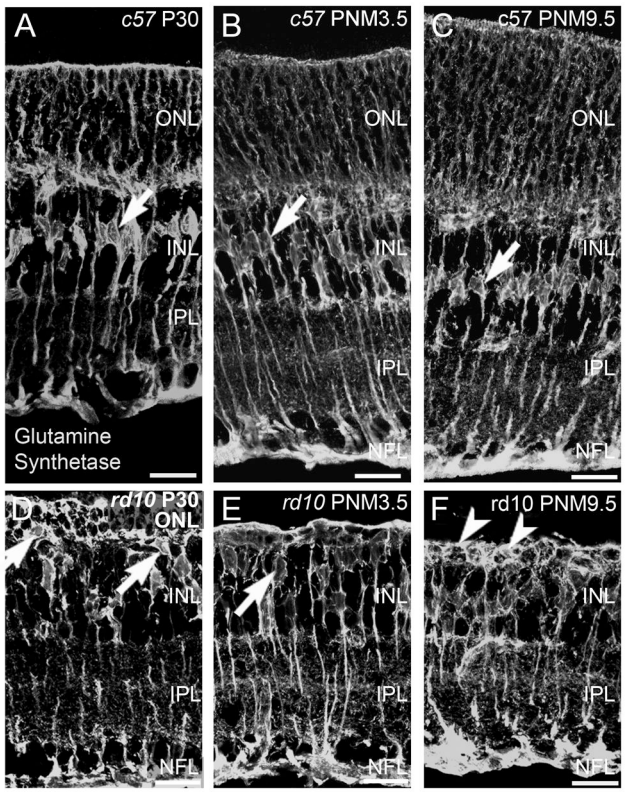

Figure 10.

Co-localization of Syntaxin 3, a ribbon synapse-specific SNARE protein, and VGluT1 is progressively reduced in photoreceptor terminals but is largely retained in bipolar cell terminals in the rd10 retina. A-C: Expression of synaptic proteins associated with the glutamatergic ribbon synaptic terminals of photoreceptors and bipolar cells in the wildtype C57BL/6 mouse retina at PNM9.5. A. Syntaxin 3 in the wildtype retina is expressed exclusively in the ynaptic terminals of photoreceptors in the OPL and bipolar cells in the IPL. B. Similarly, VGluT1 in the wildtype retina is expressed exclusively in the synaptic terminals of photoreceptors in the OPL and bipolar cells in the IPL. C. Overlay of panels A and B. D-F: Localization of ribbon synapse associated proteins in the rd10 mouse retina at PN30. D. Syntaxin 3 expression in the rd10 retina at PN30. Surviving photoreceptor terminals (arrow) continue to express syntaxin 3, although the loss of terminals from the OPL is already apparent even at this early stage of degeneration. E. Surviving photoreceptor terminals also continue to express VGluT1. F. Overlay of panels D and E. The two proteins show a high degree of co-localization in both the OPL and IPL (arrow). G-I: Localization of ribbon synapse associated proteins in the rd10 mouse retina at PNM9.5. G. Syntaxin 3 expression persists in surviving cone terminals in the OPL and bipolar cell terminals in the IPL (arrowheads). H. VGluT1 expression also persists in surviving cone terminals in the OPL and bipolar cell terminals in the IPL. I. The merged image shows co-localization of syntaxin 3 and VGluT1 labeling in surviving cone terminals, however, VGLUT1 expression is reduced compared to syntaxin 3. Bipolar cell terminals continue to show extensive co-localization of syntaxin 3 and VGluT1 in the IPL. Scale bar = 20 μm, all panels.

Table 1

List of antibodies used for immunostaining

Antigen	Immunogen	Manufacturer (catalog #)	Host	Dilution
Calbindin	rat, full length recombinant	SWANT; Bellinzona, Switzerland (CB38)	rabbit polyclonal	1 to 1000
Calbindin	chicken, full length purified from gut	SWANT; Bellinzona, Switzerland (#300)	mouse monoclonal (clone 300/301)	1 to 2000
Calretinin	guinea pig, full length purified from brain	Chemicon International, Temecula, CA (AB5054)	rabbit polyclonal	1 to 1000
GAD65	human, full length from baculovirus infected cells	Chemicon International, Temecula, CA (AB5082)	rabbit polyclonal	1 to 500
Gγ13	mouse, peptide amino acids 47–59 (FLNPDLMKNNPWV)	Dr. R. Margolskee, Mount Sinai School of Medicine New York, NY	rabbit polyclonal	1 to 500
GluR4	rat, C-terminus (RQSSGLAVIASDLP)	Chemicon International, Temecula, CA (AB1508)	rabbit polyclonal	1 to 100
GS	sheep, full length purified from brain	Chemicon International, Temecula, CA (MAB302)	mouse monoclonal (clone GS-6)	1 to 400
PKCα	human, peptide, amino acids 270–427 [1]	BD Transduction Laboratories, San Jose, CA (#610108)	mouse monoclonal (clone 3)	1 to 20 to 1:50
PKCα	rat, amino acids 659–672; C-terminal variable V5 region (RLVLASIDQADFQG)	Sigma; St Louis, MO (P4334)	rabbit polyclonal	1 to 5000
SNAP-25	human, crude synaptic immunoprecipitate	Chemicon International, Temecula, CA (MAB331)	mouse monoclonal (clone SP14)	1 to 5000
SV2 (pan)	electric ray, synaptic vesicles	Dr. K Buckley, Harvard Medical School, Boston, MA	mouse monoclonal	1 to 500
Synapsin I	sheep, full length purified from brain	Chemicon International, Temecula, CA (MAB10137)	mouse monoclonal (clone 3C5)	1 to 200
Syntaxin 3	rat, recombinant, amino acids 4–197 [2] fused to glutathione S-transferase	AbCam, Cambridge, MA (AB4113)	rabbit polyclonal	1 to 1000
Syntaxin 4	mouse, peptide, amino acids 2–23 (RDRTHELRQGDNISDDEDEVRV)	Chemicon International, Temecula, CA (AB5330)	rabbit polyclonal	1 to 100
TH	rat, full length, purified from P12 cells	Chemicon International, Temecula, CA (MAB318)	mouse monoclonal (clone LNC1)	1 to 500
VAMP2	rat, peptide, amino acids 2–17 (SATAATVPPAAPAGEG)	Synaptic Systems; Gottingen, Germany (#104–202)	rabbit polyclonal	1 to 5000
VGLUT1	rat, peptide, amino acids 541–560 (GATHSTVQPPRPPPPVRDY)	Chemicon International, Temecula, CA (AB5905)	guinea pig polyclonal	1 to 5000
VGLUT3	rat, peptide, amino acids 569–588 (FEGEEPLSYQNEEDFSETS)	Chemicon International, Temecula, CA (AB5421)	guinea pig polyclonal	1 to 3000

[1] PKCα: amino acids 270–427:
PASGWYKLLNQEEGEYYNVPIPEGDEEGNMELRQKFEKAKLGPAGNKVISPSEDRKQPSNNLDRVKLTDFNFLMVLGKGSFGKVMLADRKGTEELYAIKILKKDVVIQDDDVECTMVEKRVLALLDKPPFLTQLHSCFQTVDRLYFVMEYVNGGDLMY

[2] Syntaxin 3: amino acids 1–197: RLEQLKAKQLTQDDDTDEVEIAIDNTAFMDEFFSEIEETRLNIDKISEHVEEAKKLYSIILSAPIPEPKTKDDLEQLTTEIKKRANNVRNKLKSMEKHIEEDEVRSSADLRIRKSQHSVLSRKFVEVMTKYNEAQVDFRERSKGRIQRQLEITGKKTTDEELEEMLESGNPAIFTSGIIDSQISKQALSEIEGR

Table 2

List of abbreviations used in figure legends.

A	amacrine cell
BV	blood vessel
c57	*C57BL/6* mouse
GAD-65	glutamic acid decarboxylase 2
GCL	ganglion cell layer.
Gγ13	guanine nucleotide binding protein (G protein), gamma 13
GluR4	ionotropic glutamate receptor subunit 4
GS	glutamine synthetase
H	horizontal cell
INL	inner nuclear layer
IPL	inner plexiform layer
ONL	outer nuclear layer
OPL	outer plexiform layer
PKC	protein kinase C-α
rd10	homozygous *Pde6b*^{rd10} mouse
SV2	synaptic vesicle 2
TH	tyrosine hydroxylase
VGluT1	vesicular glutamate transporter 1
VGluT3	vesicular glutamate transporter 3